



UNIVERSITÀ DEGLI STUDI
DI TRENTO



PhD oral defense
26th March 2012

Spacetime metrology with LISA Pathfinder

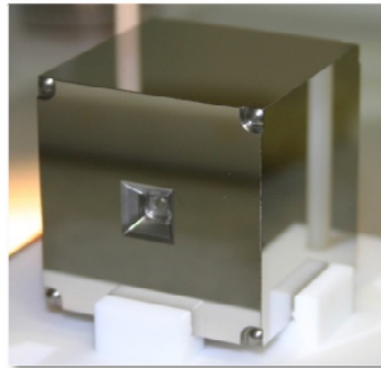
Giuseppe Congedo

Advisors: Prof. Stefano Vitale
Dr. Mauro Hueller

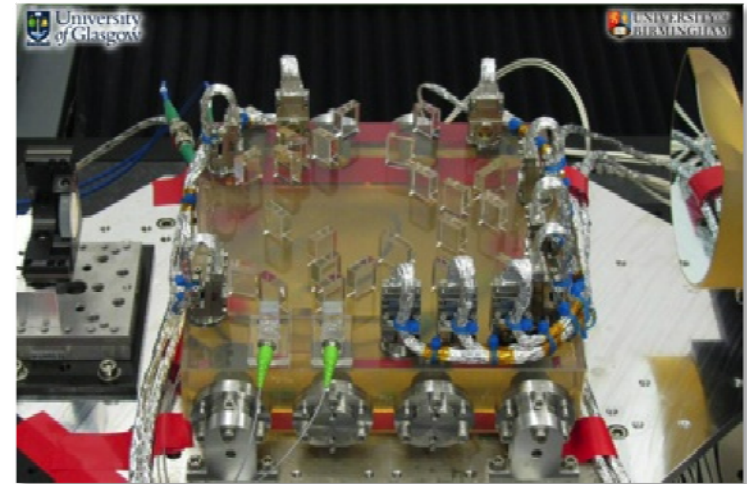
LISA Pathfinder



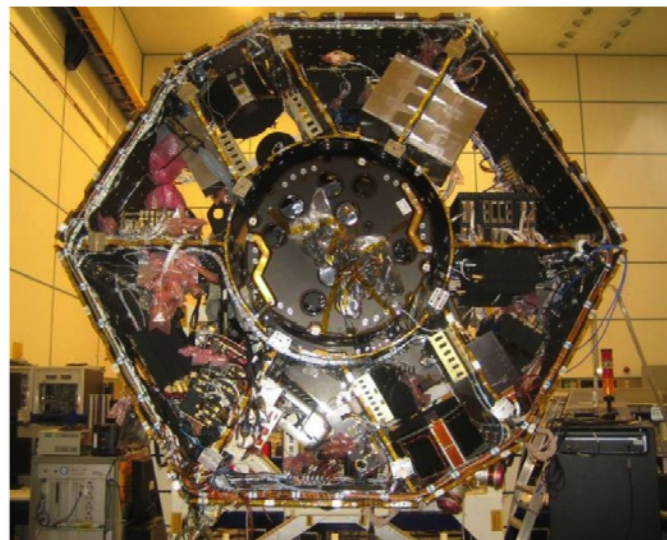
vibration tests



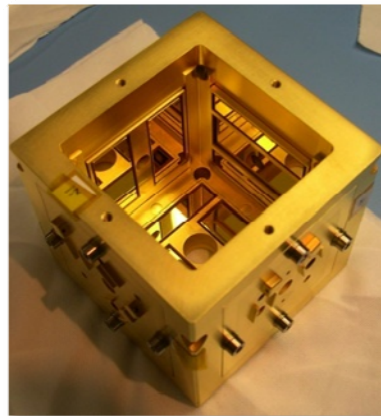
Test Mass



Optical Bench



SpaceCraft



Housing

courtesy of



- Partnership of many universities world wide
- Univ. of Trento plays the role of Principal Investigator
- Currently in the final integration
- Planned to flight in the next years

Outline of the talk

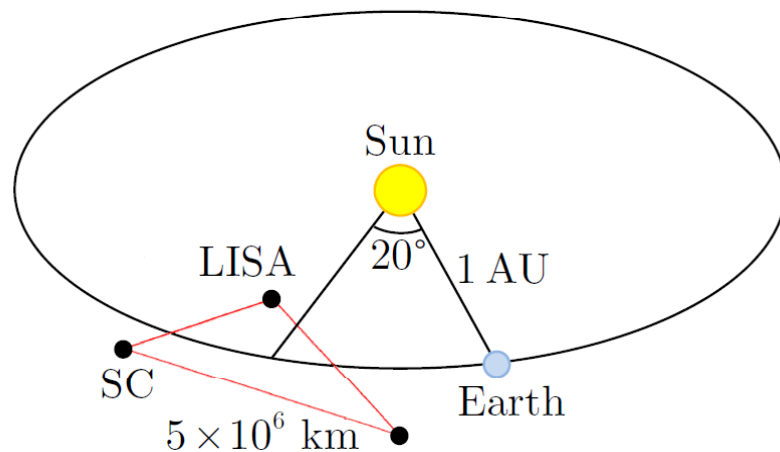
In the framework of this ESA mission, we talk about:

- Theoretical characterization of the LISA arm *without/with* noise
- Dynamical modeling for LISA Pathfinder, closed-loop equations of motion
- Data analysis: simulation and analysis of some experiments, system calibration, estimation of the acceleration noise, ...

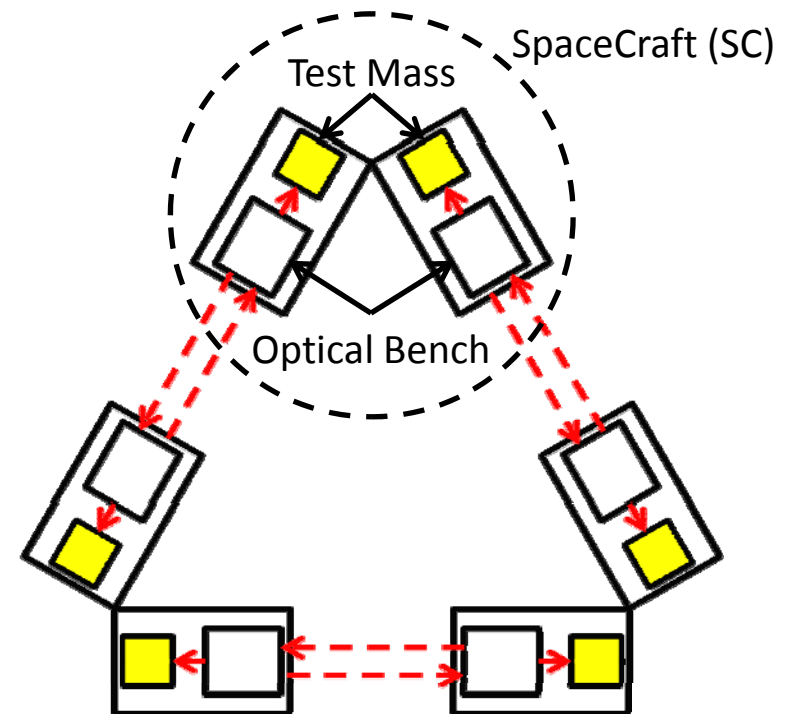
LISA, a space-borne GW detector

LISA is the proposed ESA-NASA mission for GW astrophysics in 0.1 mHz – 0.1 Hz

- astrophysical sources at cosmological distances
- merger of SMBHs in galactic nuclei
- galactic binaries (spatially resolved and unresolved)
- EMRIs
- GW cosmic background radiation

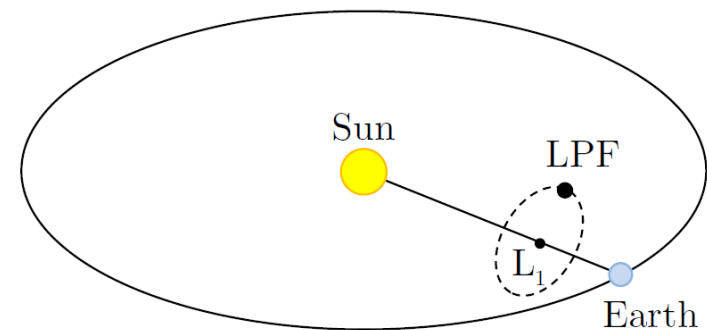
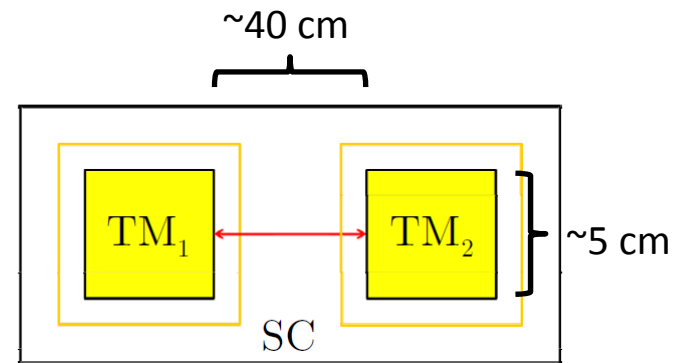


LISA measures the **relative velocities** between the Test Masses (TMs) as **Doppler frequency shifts**

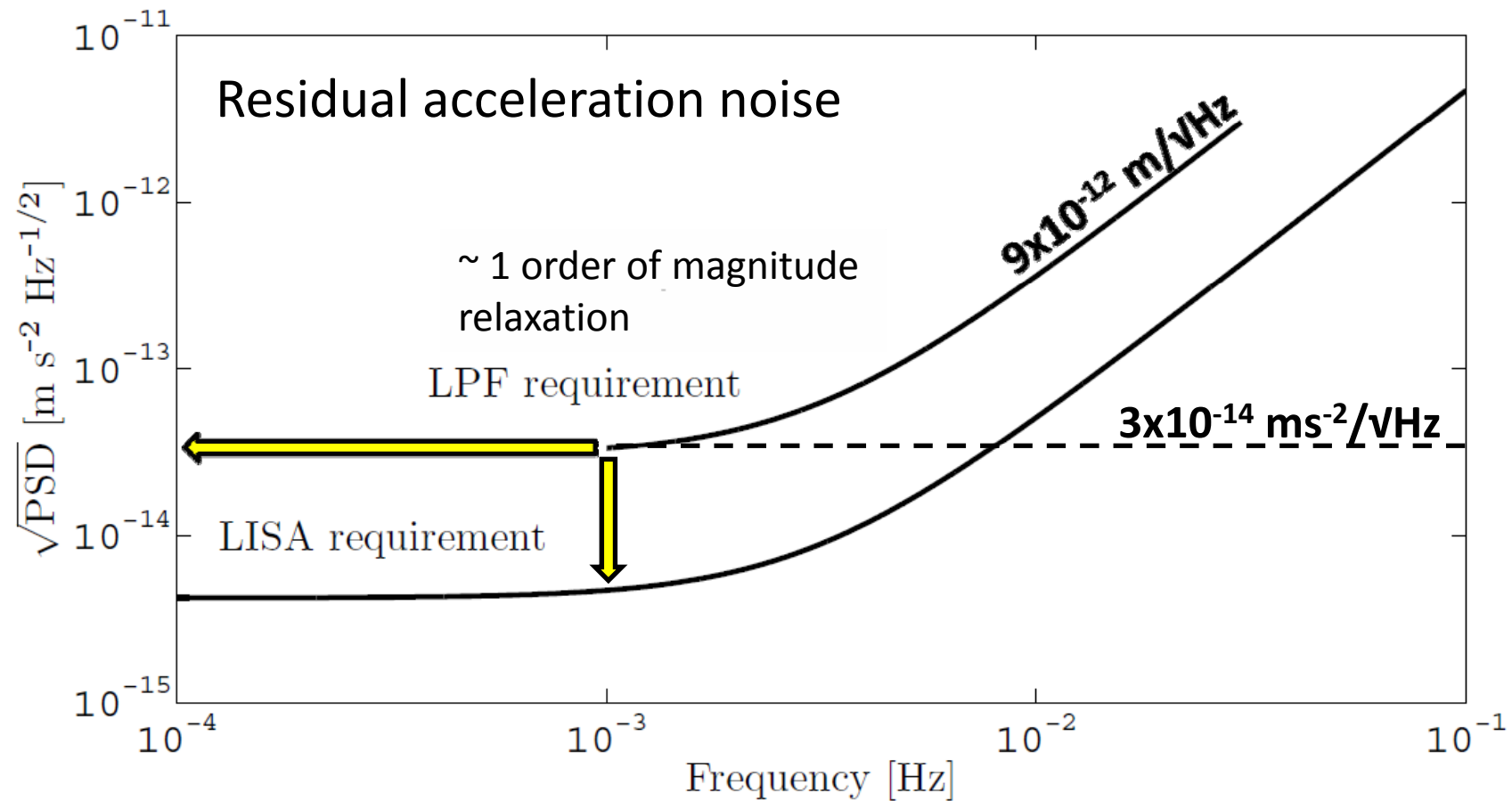


LISA Pathfinder, in-flight test of geodesic motion

- **Down-scaled version of LISA arm**
~40 cm
- In-flight test of the LISA hardware (sensors, actuators and controllers)
- Prove geodesic motion of TMs to within **$3 \times 10^{-14} \text{ ms}^{-2}/\sqrt{\text{Hz}}$ @1mHz** *differential acceleration noise requirement*
- Optically track the relative motion to within **$9 \times 10^{-12} \text{ m}/\sqrt{\text{Hz}}$ @1mHz** *differential displacement noise*



LISA Pathfinder, in-flight test of geodesic motion



Spacetime metrology without noise

How does the LISA arm work?

It is well-known in General Relativity that the Doppler frequency shift measured between an emitter sending photons to a receiver – we name it **Doppler link** – is

$$\delta\omega_{e\rightarrow r} = k_\mu \Delta v_{e\rightarrow r}^\mu$$

The **differential operator** implementing the parallel transport of the emitter 4-velocity along the photon geodesic can be defined as

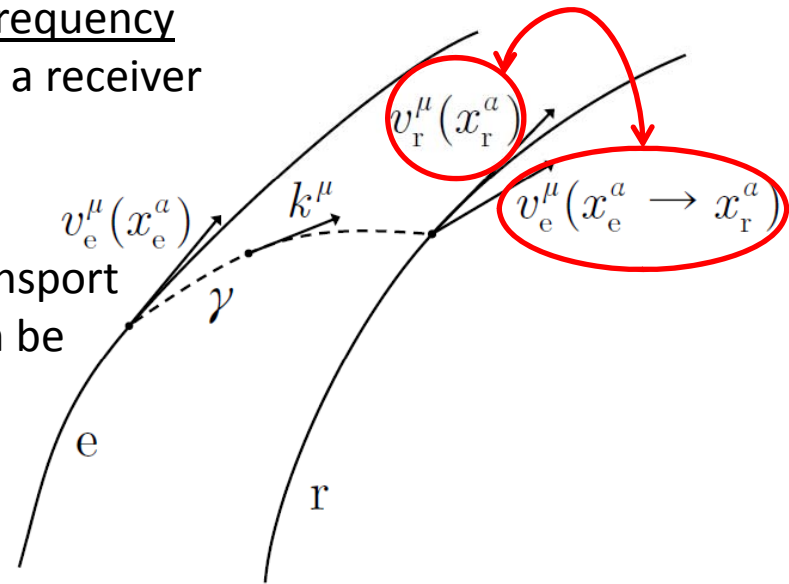
$$\Delta v_{e\rightarrow r}^\mu = v_r^\mu(x_r^\alpha) - v_e^\mu(x_e^\alpha \xrightarrow{\text{parallel}} x_r^\alpha)$$

and one can show that it is given by

$$\Delta v_{e\rightarrow r}^\mu = \delta v_{e\rightarrow r}^\mu + \int_\gamma \Gamma_{\alpha\beta}^\mu v_e^\alpha dx^\beta$$

The Doppler link measures

- **relative velocity** between the particles (without parallel transport)
- the integral of the **affine connection** (i.e., curvature + gauge effects)



Doppler link as differential accelerometer

For low velocities and *along the optical axis*, differentiating the Doppler link it turns out

$$\delta\omega_{e \rightarrow r} = k_\mu \Delta v_{e \rightarrow r}^\mu \xrightarrow{d/d\tau} \delta\dot{\omega}_{e \rightarrow r} = k_\mu \delta a_{e \rightarrow r}^\mu + k_\mu \int_\gamma \frac{d\Gamma_{\alpha\beta}^\mu}{d\tau} v_e^\alpha dx^\beta$$

$\sim \omega/c (1,1,0,0)$
 \downarrow
 \uparrow
 $\sim (c,0,0,0)$
 to 1st order

The Doppler link (and the LISA arm) can be reformulated as a

differential time-delayed accelerometer

measuring:

- The spacetime curvature along the beam $\delta a_R = c^2 \int_\gamma R_{0110} dx$
- Parasitic differential accelerations $k_\mu \delta a_{e \rightarrow r}^\mu$
- Gauge “non-inertial” effects $\delta a_{\text{gauge}} = \frac{1}{2} c^2 \int_\gamma (h_{00,00} + 2h_{01,00} + 2h_{01,01} - h_{00,11}) dx$

Doppler response to GWs in the weak field limit

To prove that this reasoning is correct, it is possible to evaluate the Doppler response to GWs in the TT gauge

$$h_{\mu\nu} = \begin{pmatrix} 0 & \dots & 0 \\ \vdots & h_+ & h_\times & \vdots \\ 0 & \dots & 0 \end{pmatrix}$$

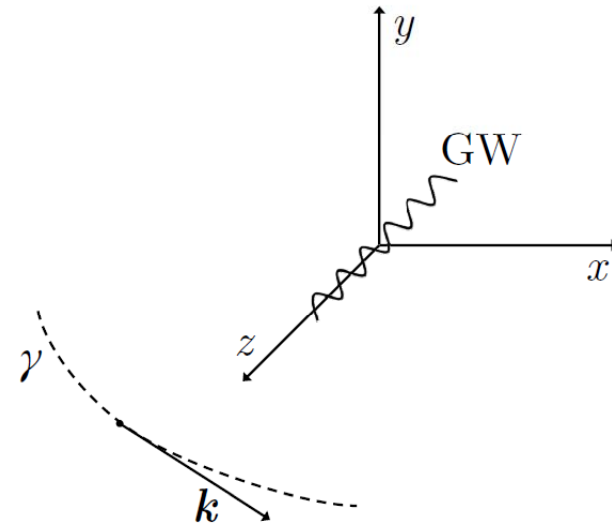
obtaining the standard result already found in literature

$$\frac{\delta\omega_h}{\omega_e} = \frac{1}{2} [h(t) - h(t - \delta x/c)]$$

where h is the “convolution” with the directional sensitivities and the GW polarizations

$$h(t, \theta, \phi) = \xi_+(\theta, \phi)h_+(t) + \xi_\times(\theta, \phi)h_\times(t)$$

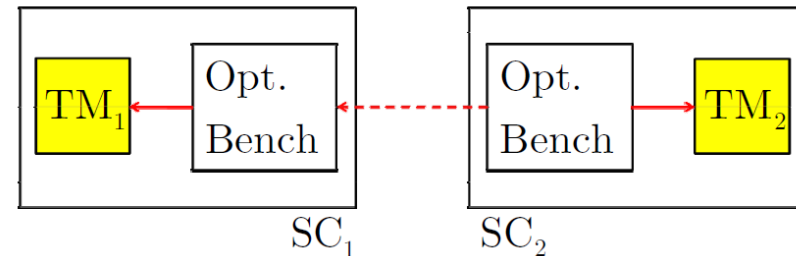
The parallel transport induces a **time delay** to the time of the emitter



Noise sources within the LISA arm

- LPF is a down-scaled version of the LISA arm, which is a sequence of 3 measurements:

$$\frac{\delta\omega_{2 \rightarrow 1}}{\omega_e} = \frac{1}{c} \hat{\mathbf{k}} \cdot \left(\delta\mathbf{v}_{SC} + \mathbf{v}_{TM_2}^{(SC)} - \mathbf{v}_{TM_1}^{(SC)} \right)$$



- In LISA there are 3 main noise sources:
 - laser frequency noise from armlength imbalances, compensated by TDI, not present in LPF
 - parasitic differential accelerations, characterized with LPF
 - sensing noise (photodiode readout), characterized with LPF

Laser frequency noise

In space, laser frequency noise can not be suppressed as on-ground: arm length imbalances of a few percent produce an unsuppressed frequency noise of

$10^{-13}/\text{VHz}$ ($2 \times 10^{-7} \text{ ms}^{-2}/\text{VHz}$) @1mHz

Doppler links

$$\sigma_k(t) = s_k(t) + S_k(t) - s'_{p[k]}(t - T_{p^2[k]})$$

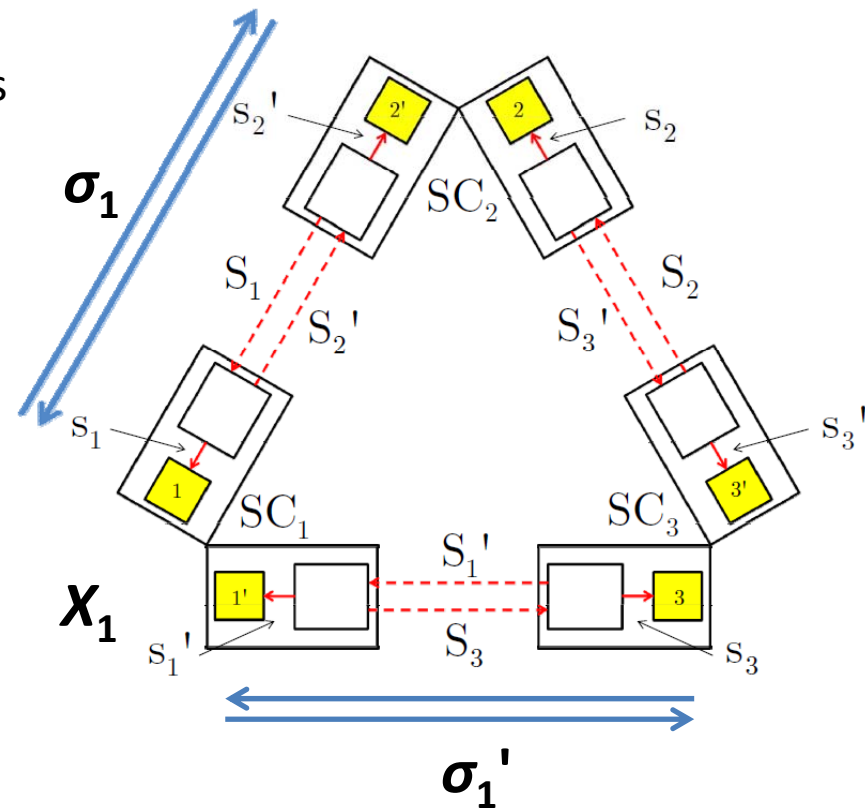
$$\sigma'_k(t) = s'_k(t) + S'_k(t) - s_{p^2[k]}(t - T_{p[k]})$$

Time-Delay Interferometry (TDI) suppresses the frequency noise to within

$10^{-20}/\text{VHz}$ ($2 \times 10^{-15} \text{ ms}^{-2}/\text{VHz}$) @1mHz

It is based upon **linear combinations of properly time delayed Doppler links**

$$X_k(t) = \sigma'_k(t) + \sigma_{p^2[k]}(t - T_{p[k]}) + \sigma_k(t - 2T_{p[k]}) + \sigma'_{p[k]}(t - T_{p^2[k]} - 2T_{p[k]}) \\ - [\sigma_k(t) + \sigma'_{p[k]}(t - T_{p^2[k]}) + \sigma'_k(t - 2T_{p^2[k]}) + \sigma_{p^2[k]}(t - T_{p[k]} - 2T_{p^2[k]})]$$



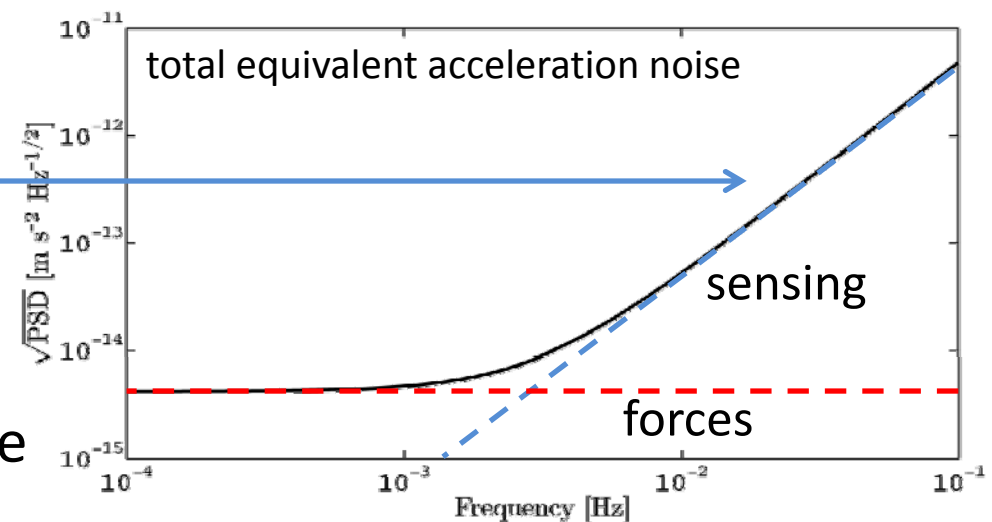
Total equivalent acceleration noise

- Differential forces (per unit mass) between the TMs, due to electromagnetics & self-gravity within the SC, $S_{n,\delta f/m}(\omega)$
- Sensing noise (readout, optical bench misalignments), $S_{n,\delta x}(\omega)$

We can express all terms as **total equivalent acceleration noise**

$$S_{n,\delta a}(\omega) = S_{n,\delta f/m}(\omega) + \omega^4 S_{n,\delta x}(\omega)$$

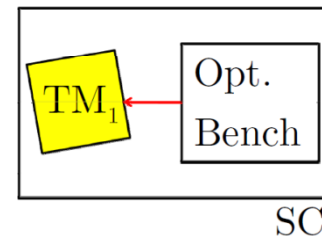
will be demonstrated by LPF to be within $3 \times 10^{-14} \text{ ms}^{-2}/\sqrt{\text{Hz}}$ @1mHz



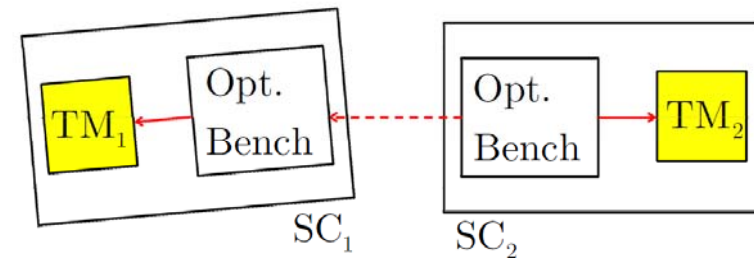
Dynamics of fiducial points

- **Fiducial points** are the locations on TM surface where light reflects on
- They do not coincide with the centers of mass
- As the TMs are not pointlike, extended body dynamics couples with the differential measurement (cross-talk)

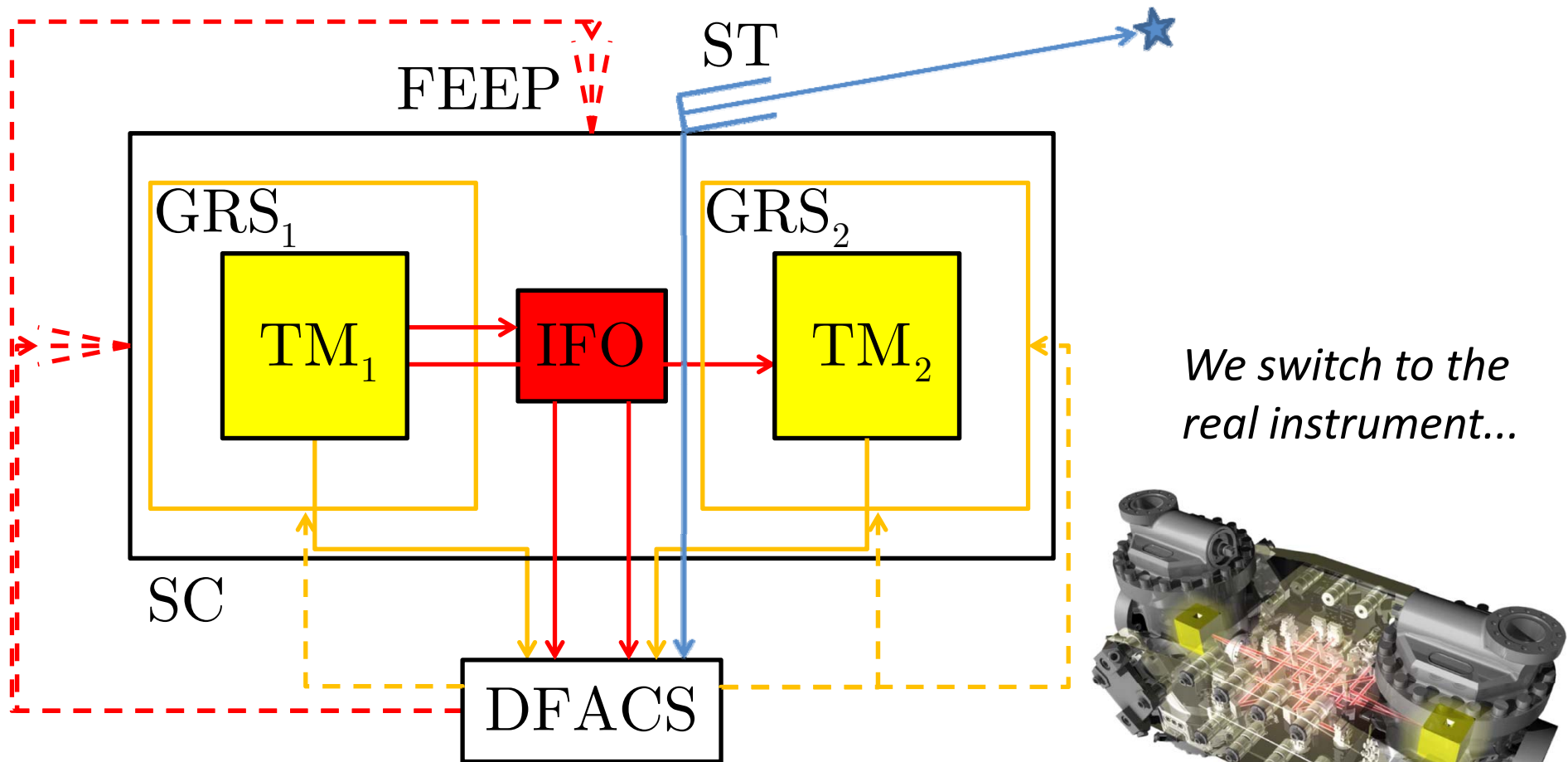
Local link



Link between the SCs

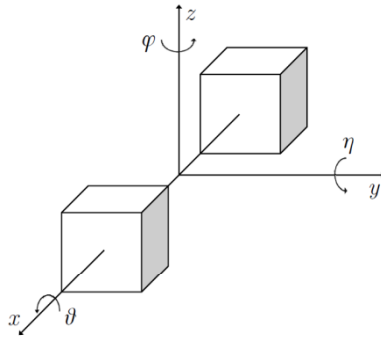


LISA Technology Package



15 control laws are set up to minimize:
SC jitter and **differential force disturbances**

Degrees of freedom



Science mode, along the optical axis x :

- TM_1 is in **free fall**
- the SC is forced to follow TM_1 through **thruster actuation**
- TM_2 is forced to follow TM_1 through **capacitive actuation**

Coordinate	Control	Sensor	Actuator
x_1	Drag-free	$o_1 = \text{IFO}[x_1]$	FEEP
y_1	Drag-free	$o_{y_1} = \text{GRS}[y_1]$	FEEP
z_1	Drag-free	$o_{z_1} = \text{GRS}[z_1]$	FEEP
θ_1	Drag-free	$o_{\theta_1} = \text{GRS}[\theta_1]$	FEEP
η_1	Elect. suspension	$o_{\eta_1} = \text{IFO}[\eta_1]$	GRS
ϕ_1	Elect. suspension	$o_{\phi_1} = \text{IFO}[\phi_1]$	GRS
x_2	Elect. suspension	$o_{12} = \text{IFO}[x_{12}]$	GRS
y_2	Drag-free	$o_{y_2} = \text{GRS}[y_2]$	FEEP
z_2	Drag-free	$o_{z_2} = \text{GRS}[z_2]$	FEEP
θ_2	Elect. suspension	$o_{\theta_2} = \text{GRS}[\theta_2]$	GRS
η_2	Elect. suspension	$o_{\eta_{12}} = \text{IFO}[\eta_{12}]$	GRS
ϕ_2	Elect. suspension	$o_{\phi_{12}} = \text{IFO}[\phi_{12}]$	GRS
θ_{SC}	Attitude	$o_{\theta_{SC}} = \text{ST}[\theta_{SC}]$	GRS
η_{SC}	Attitude	$o_{\eta_{SC}} = \text{ST}[\eta_{SC}]$	GRS
ϕ_{SC}	Attitude	$o_{\phi_{SC}} = \text{ST}[\phi_{SC}]$	GRS

Closed-loop dynamics

In LPF dynamics:

- the relative motion is expected to be within \sim nm
- we neglect non-linear terms from optics and extended body Euler dynamics
- the forces can be expanded to linear terms

Since the linearity of the system, it follows that the equations of motion are linear, hence in frequency domain they can be expressed in matrix form (for many dofs)

$$\begin{aligned}\ddot{x} &= g(x, t) \Rightarrow \\ \ddot{x} &= g_0 - kx + \dots \Rightarrow \\ \underbrace{(d^2 / dt^2 + k)}_{\text{Dynamics operator}} x &= g_0\end{aligned}$$

Closed-loop dynamics

As said, the equations of motion are linear and can be expressed in matrix form

Dynamics $D \dot{q} = g$ “forces produce the motion”

Sensing $o = S q + o_n$ “positions are sensed”

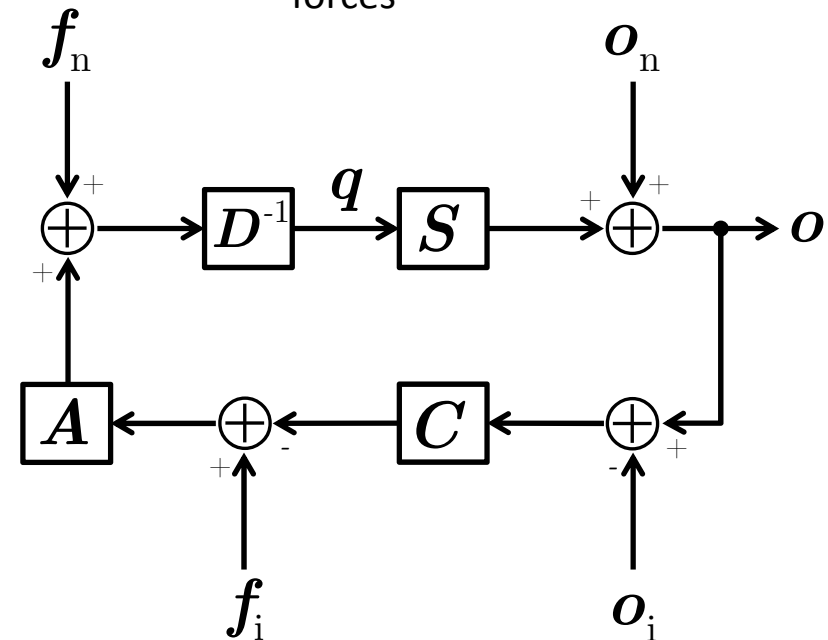
Control $g = f_n + A [f_i - C (o - o_i)]$ “noise, actuation and control forces”

The *generalized* equation of motion in the sensed coordinates

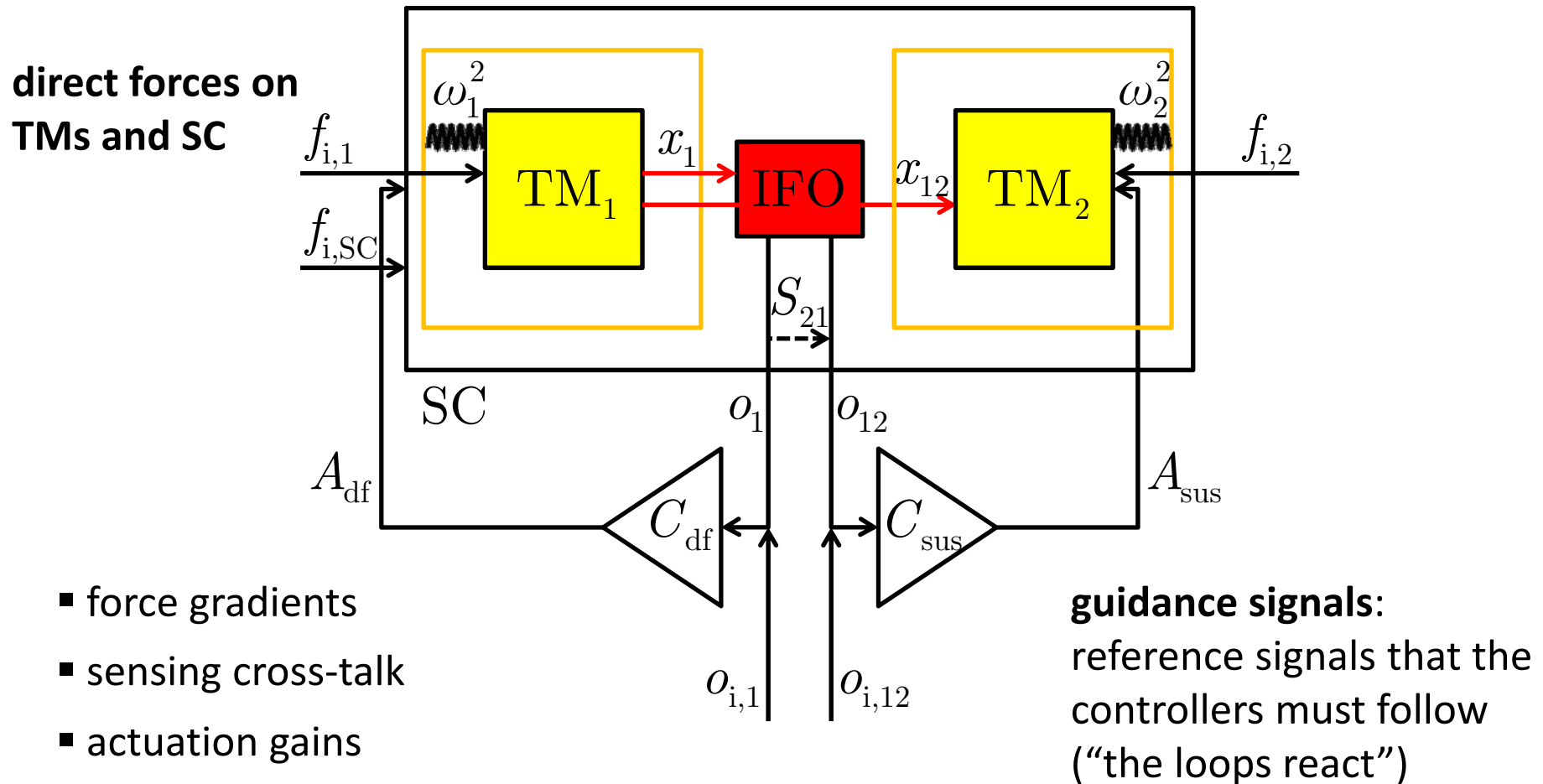
$$\Delta o = f_n + D S^{-1} o_n + A (f_i + C o_i)$$

where the 2nd-order differential operator is defined by

$$\Delta = D S^{-1} + A C$$



Dynamical model along the optical axis



Dynamical model along the optical axis

The model along x can be mapped to the matrix formalism...

$$\begin{aligned}
 s^2 x_1 + s^2 x_{SC} + \omega_1^2 x_1 + \Gamma_x (x_2 - x_1) &= f_1 \\
 s^2 x_2 + s^2 x_{SC} + \omega_2^2 x_2 - \Gamma_x (x_2 - x_1) &= f_2 - C_{sus}(s) o_{12} \\
 s^2 x_{SC} - \tilde{m}_1 \omega_1^2 x_1 - \tilde{m}_2 \omega_2^2 x_2 &= f_{SC} + C_{df}(s) o_1 \\
 &\quad - \tilde{m}_1 f_1 - \tilde{m}_2 f_2 \\
 &\quad + \tilde{m}_2 C_{sus}(s) o_{12}
 \end{aligned}$$

$$q = \begin{pmatrix} x_1 \\ x_{12} \end{pmatrix} \xrightarrow{S = \begin{pmatrix} 1 & 0 \\ S_{21} & 1 \end{pmatrix}} o = \begin{pmatrix} o_1 \\ o_{12} \end{pmatrix}$$

$$q = \begin{pmatrix} x_1 \\ x_{12} \end{pmatrix} \xrightarrow{D = \begin{pmatrix} s^2 + (1 + \tilde{m}_1 + \tilde{m}_2) \omega_1^2 + \tilde{m}_2 \omega_{12}^2 & \Gamma_x + \tilde{m}_2 (\omega_1^2 + \omega_{12}^2) \\ \omega_{12}^2 & s^2 + \omega_1^2 + \omega_{12}^2 - 2\Gamma_x \end{pmatrix}} g = \begin{pmatrix} (1 + \tilde{m}_1 + \tilde{m}_2) f_1 + \tilde{m}_2 f_{12} - f_{SC} - C_{df}(s) o_1 - \tilde{m}_2 C_{sus}(s) o_{12} \\ f_{12} - C_{sus}(s) o_{12} \end{pmatrix}$$

$$o = \begin{pmatrix} o_1 \\ o_{12} \end{pmatrix} \xrightarrow{C = \begin{pmatrix} C_{df}(s) & \tilde{m}_2 C_{sus}(s) \\ 0 & C_{sus}(s) \end{pmatrix}}$$

Two operators

The differential operator

$$T_{o \rightarrow f} = \Delta$$

- estimates the **out-of-loop equivalent acceleration** from the sensed motion
- subtracts known force **couplings, control forces** and **cross-talk**
- subtracts **system transients**

The transfer operator

$$T_{o_i \rightarrow o} = \Delta^{-1} A C$$

- solves the **equation of motion** for applied control bias signals
- is employed for system calibration, i.e. **system identification**

Suppressing system transients

The dynamics of LPF (in the sensed coordinates) is described by the following linear differential equation

$$\Delta o = f$$
$$\Delta o_s = f \qquad \Delta o_t = 0$$

Particular solution (*steady state*):

- depends on the *applied forces*
- can be solved in frequency domain

Homogeneous solution (*transient state*):

- depends on *non-zero initial conditions*
- is a combination of basis functions $o_t = \sum_k c_k \phi_k$

Suppressing system transients

Applying the operator on the sensed coordinates, transients are suppressed in the estimated equivalent acceleration

$$\begin{aligned}\Delta o &= \Delta (o_s + o_t) \\ &= \Delta o_s + \sum_k c_k \Delta \phi_k = f\end{aligned}$$

But, imperfections in the knowledge of the operator (imperfections in the system parameters) produce **systematic errors** in the recovered equivalent acceleration

$$\delta f = \delta \Delta (o_s + o_t)$$

System identification helps in mitigating the effect of transients

Cross-talk from other degrees of freedom

Beyond the dynamics along the optical axis...

$$o \simeq o_0 + \delta o$$

← cross-talk from other DOFs

↑ nominal dynamics along x

All operators can be expanded to first order as “imperfections” to the nominal dynamics along x

To first order, we consider only the cross-talk from a DOF to x , and not between other DOFs.

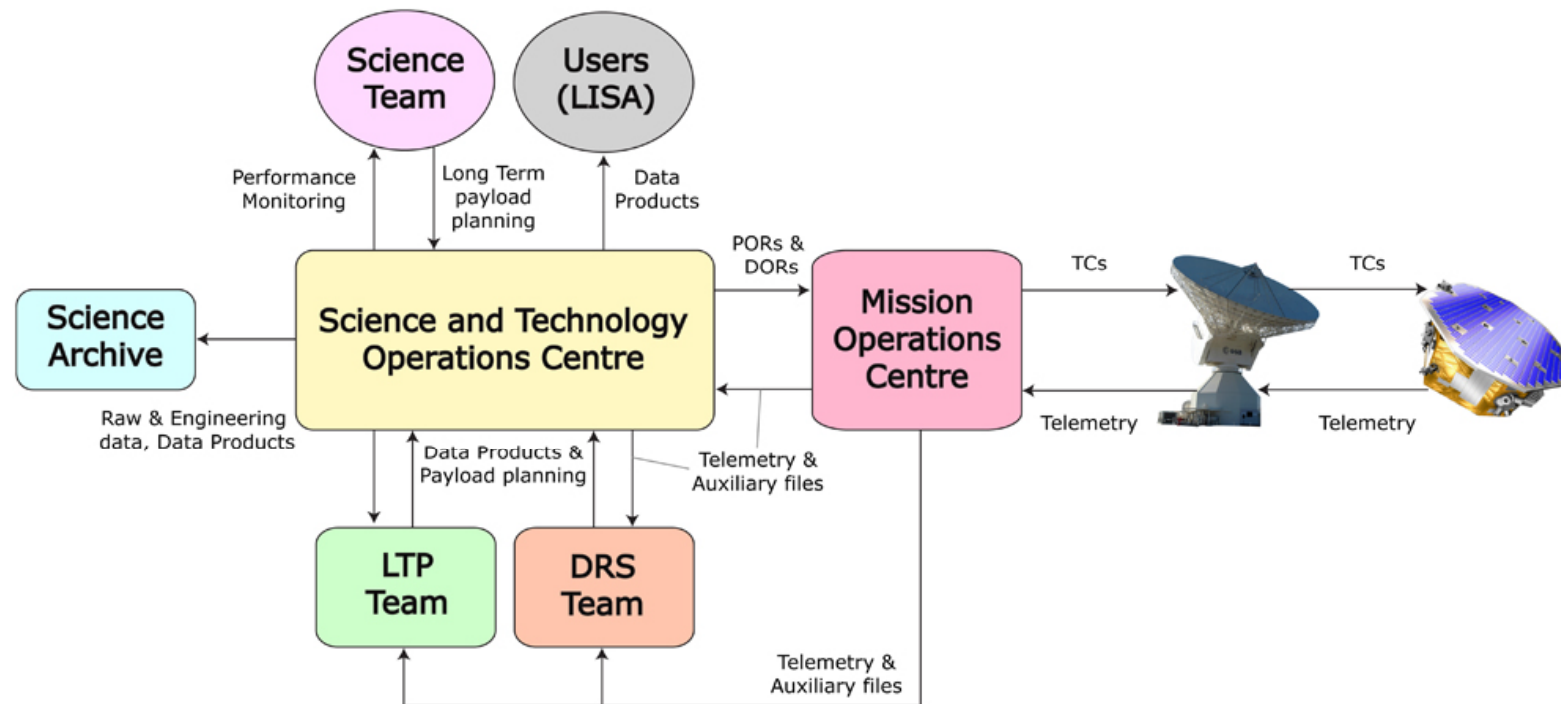
Cross-talk equation of motion

$$\Delta_0 \delta o \simeq \delta T_{f_n \rightarrow f} f_n + \delta T_{o_n \rightarrow f} o_n + \delta T_{f_i \rightarrow f} f_i + \delta T_{o_i \rightarrow f} o_i$$

Data analysis during the mission

The **Science and Technology Operations Centre (STOC)**:

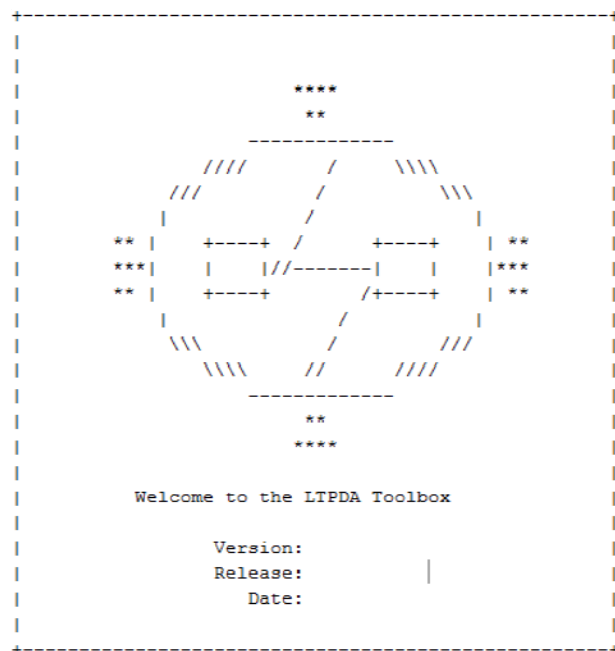
- interface between the LTP team, science community and Mission Operations
- telecommands for strong scientific interface with the SpaceCraft
- quick-look data analysis



Data analysis during the mission

Data for this thesis were simulated with both **analytical simplified models** and the **Off-line Simulation Environment** – a simulator provided by ASTRIUM for ESA.

It is realistic as it implements the same controllers, actuation algorithms and models a 3D dynamics with the couplings between all degrees of freedom



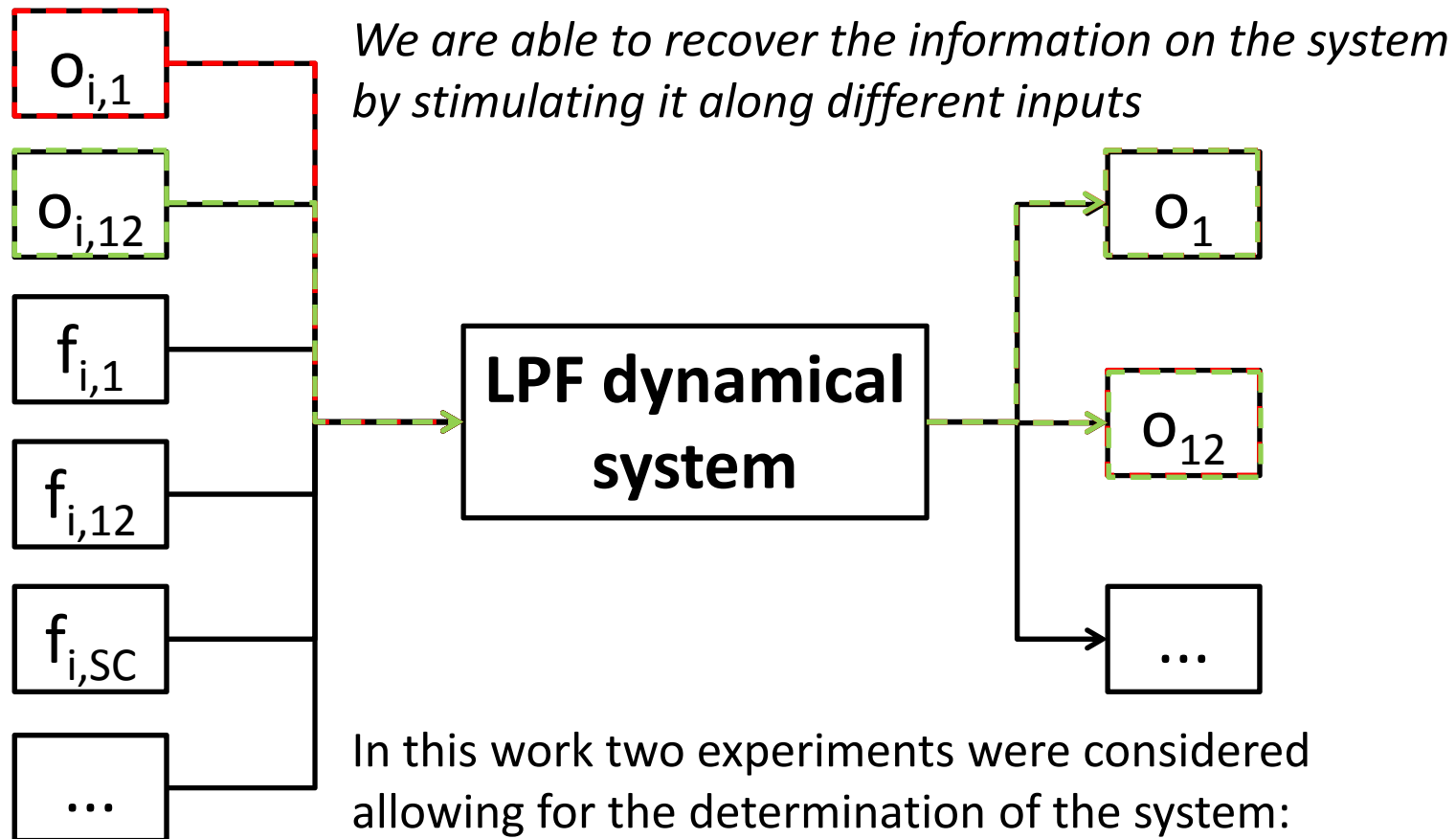
initial splash screen

During operational exercises, the simulator is employed to:

- check the **mission timeline** and the experiments
- validate the **noise budget** and **models**
- check the procedures: **system identification**, **estimation of equivalent acceleration**, etc.

Data were analyzed with the **LTP Data Analysis Toolbox** – an object-oriented Matlab environment for accountable and reproducible data analysis.

Multi-input/Multi-Output analysis



In this work two experiments were considered allowing for the determination of the system:

Exp. 1: injection into drag-free loop

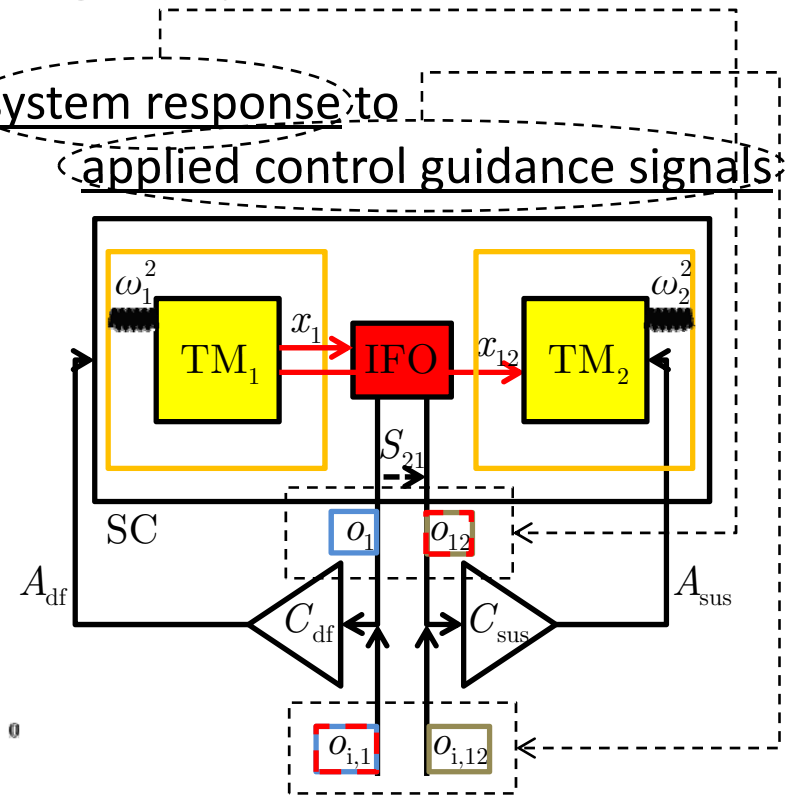
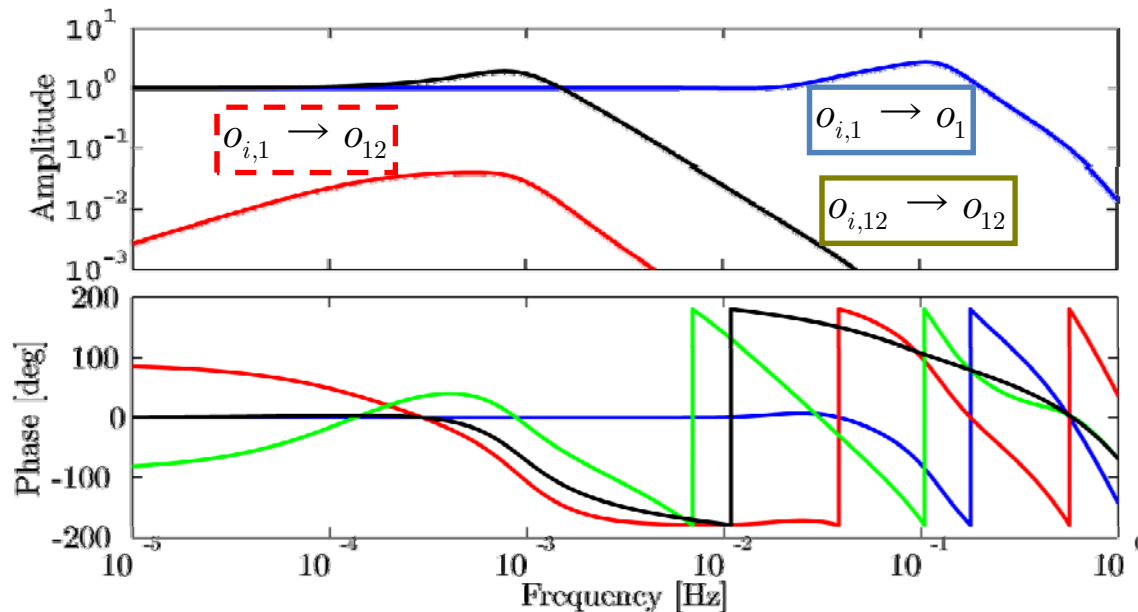
Exp. 2: injection into elect. suspension loop

LPF model along the optical axis

- For simulation and analysis, we employ a model along the optical axis

- Transfer matrix (amplitude/phase) modeling the system response to

applied control guidance signals



“the spacecraft moves”: drag-free loop

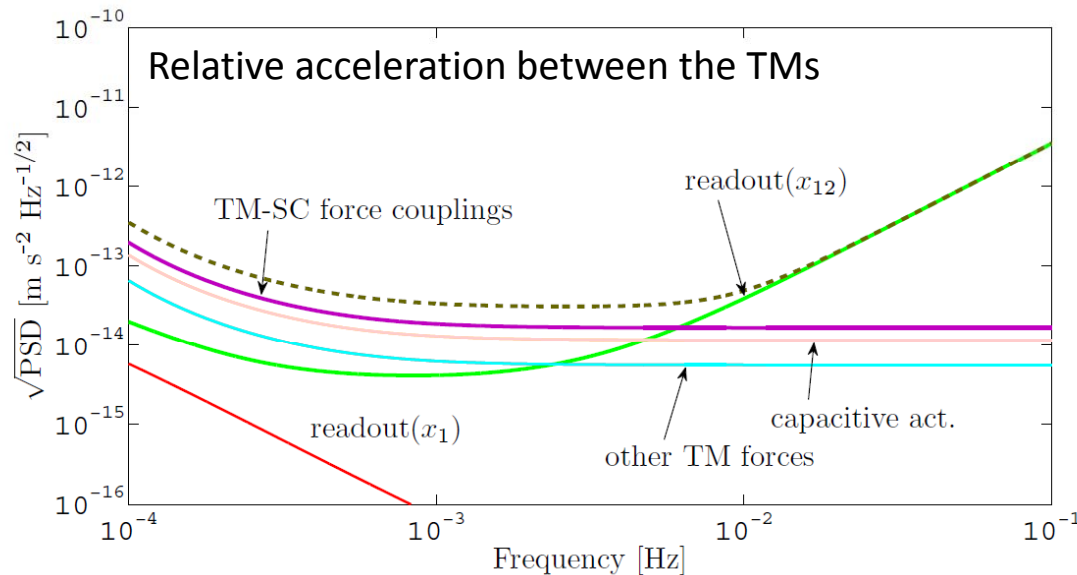
“the second test mass moves”: suspension loop

cross-talk

LPF parameters along the optical axis

Parameter	Typical value	Description
ω_1^2	$-1 \times 10^{-6} \text{ s}^{-2}$	Parasitic stiffness constant: force gradient (per unit mass) between the TM and the SC
$\omega_{12}^2 = \omega_2^2 - \omega_1^2$	$< 1 \times 10^{-6} \text{ s}^{-2}$	Differential parasitic stiffness constant: force gradient (per unit mass) between the TMs
S_{21}	1×10^{-4}	sensing cross-talk from o_1 to o_{12}
A_{df}	1	thruster actuation gain: how forces on SC translate into real applied forces
A_{sus}	1	capacitive actuation gain: how forces on TM ₂ translate into real applied forces
Δt_1	$< 1 \text{ s}$	delay in the application of the o_1 control bias
Δt_2	$< 1 \text{ s}$	delay in the application of the o_{12} control bias

Equivalent acceleration noise



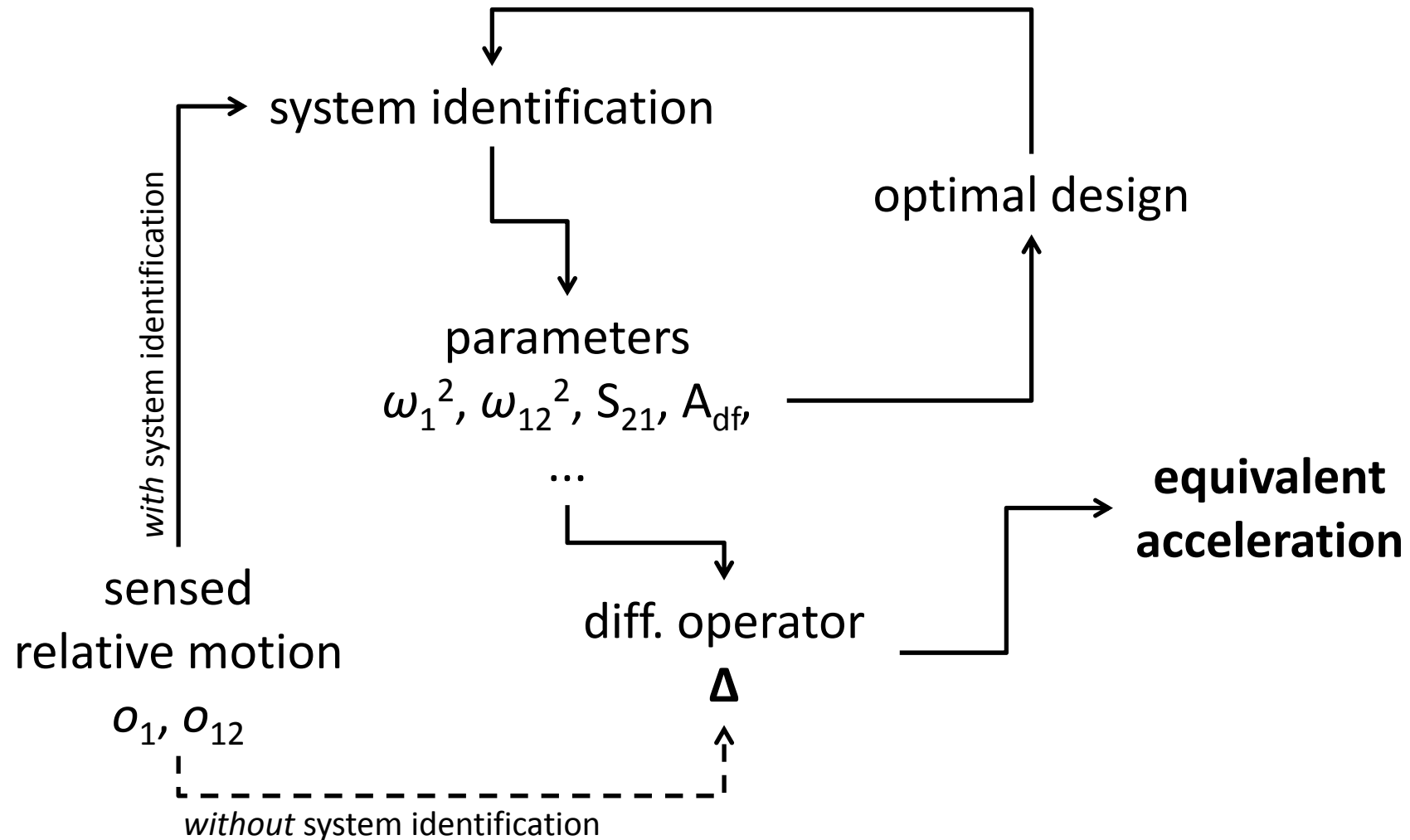
Current best estimates of the direct forces from on-ground measurements

Diff. acc. source	$\times 10^{-14} \text{ ms}^{-2}/\sqrt{\text{Hz}}$
Actuation	0.75
Brownian	0.72
Magnetics	0.28
Stray voltages	0.11

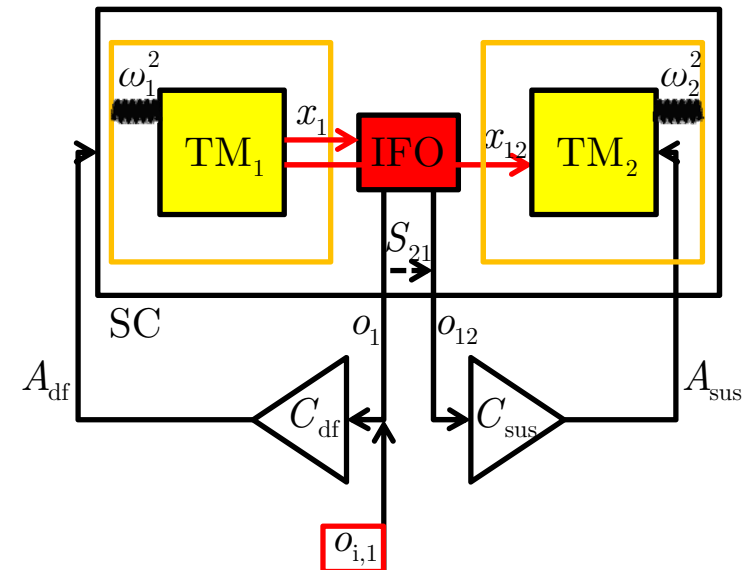
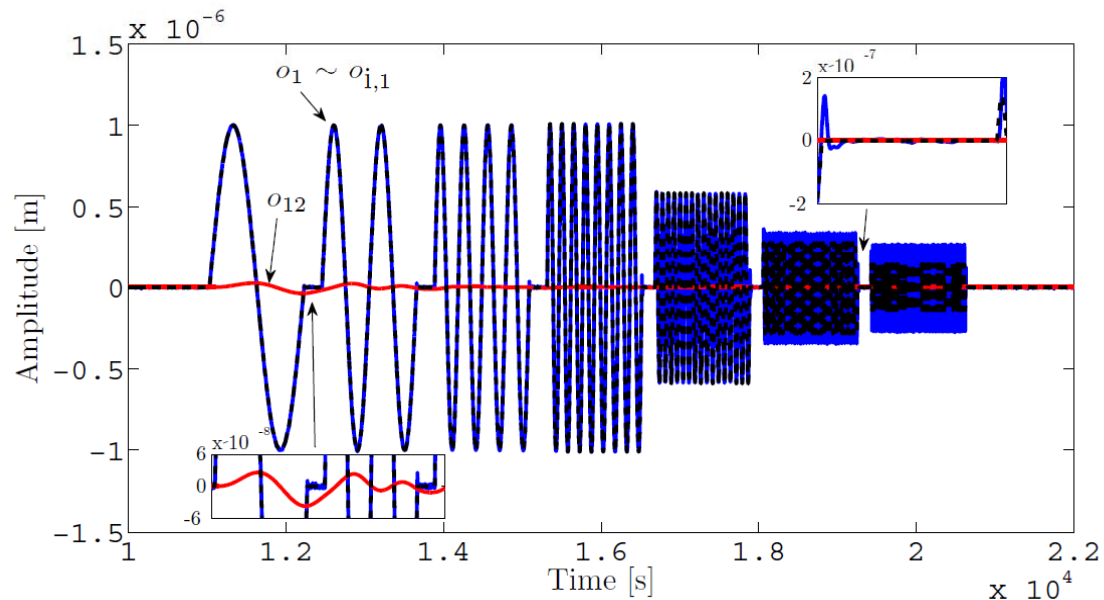
- at high frequency, dominated by sensing
- at low frequency, dominated by direct forces

Goal: prove the relevance of **system identification** for the correct assesement of the **equivalent acceleration noise**

Estimation of equivalent acceleration noise



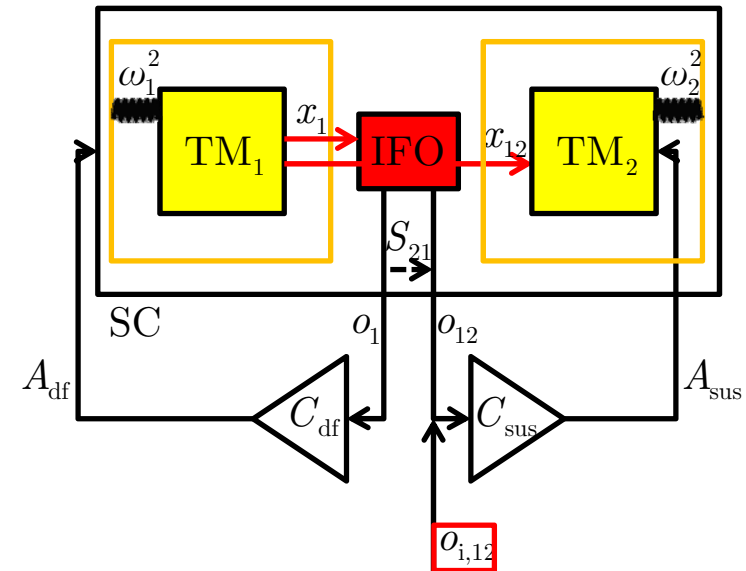
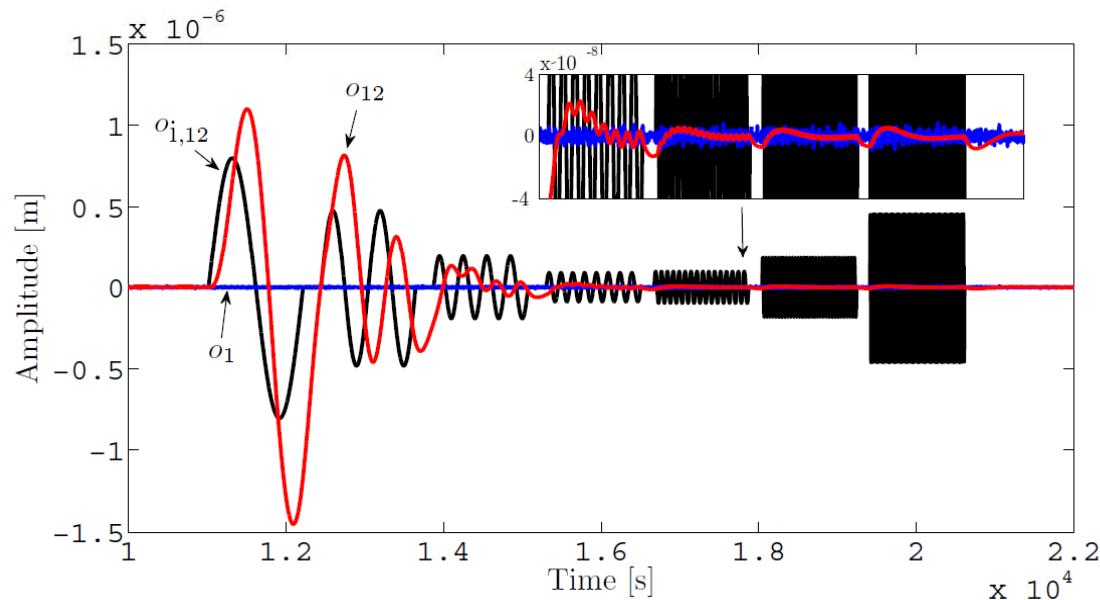
Identification experiment #1



Exp. 1: injection of sine waves into $o_{i,1}$

- injection into $o_{i,1}$ produces thruster actuation
- o_{12} shows dynamical cross-talk of a few 10^{-8} m
- allows for the identification of: A_{df} , ω_1^2 , Δt_1

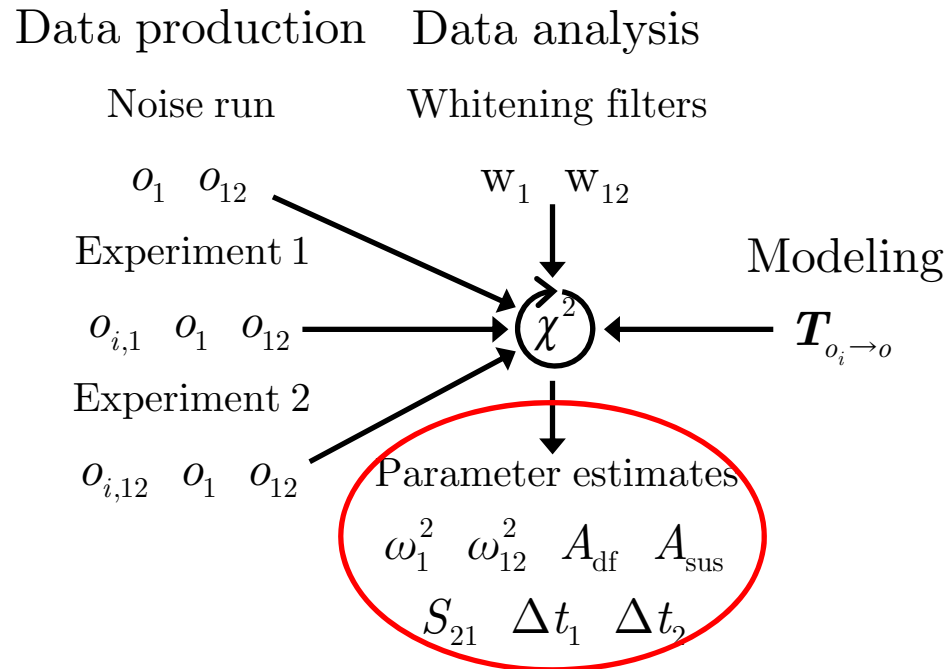
Identification experiment #2



Exp. 2: injection of sine waves into $o_{i,12}$

- injection into $o_{i,1}$ produces capacitive actuation on TM_2
- o_1 shows negligible signal
- allows for the identification of: A_{sus} , ω_{12}^2 , Δt_2 , S_{21}

Parameter estimation



Non-linear optimization:

- **preconditioned conjugate gradient search** explores the parameter space to large scales
- **derivative-free simplex** improves the numerical accuracy locally

Method extensively validated through Monte Carlo simulations

Joint (multi-experiment/multi-outputs) **log-likelihood** for the problem

$$\chi^2(p) = \int o_r(\omega, p)^* S_n(\omega)^{-1} o_r(\omega, p) d\omega$$

\uparrow \uparrow cross-PSD matrix
 $o_r(\omega, p) = o_{exp}(\omega) - T_{o_i \rightarrow o}(\omega, p) o_i(\omega)$
 residuals

Non-Gaussianities

Investigated the case of non-gaussianities (glitches) in the readout producing fat tails in the statistics (strong excess kurtosis)

Regularize the log-likelihood with a weighting function

$$\chi^2 = \sum_i \rho(r_{w,i})$$

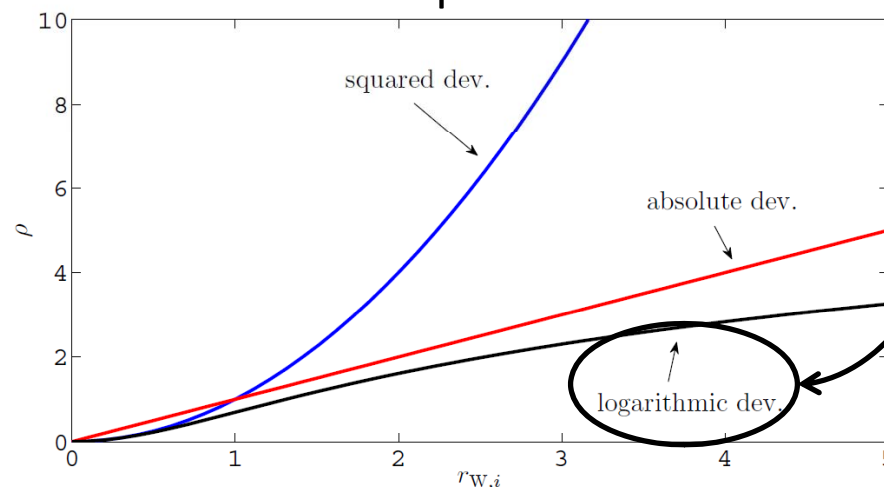
$$\rho(r_{w,i}) = \begin{cases} r_{w,i}^2 \\ |r_{w,i}| \\ \log(1 + r_{w,i}^2) \end{cases}$$

mean squared dev. (aka, "ordinary least squares"), Gaussian distr.

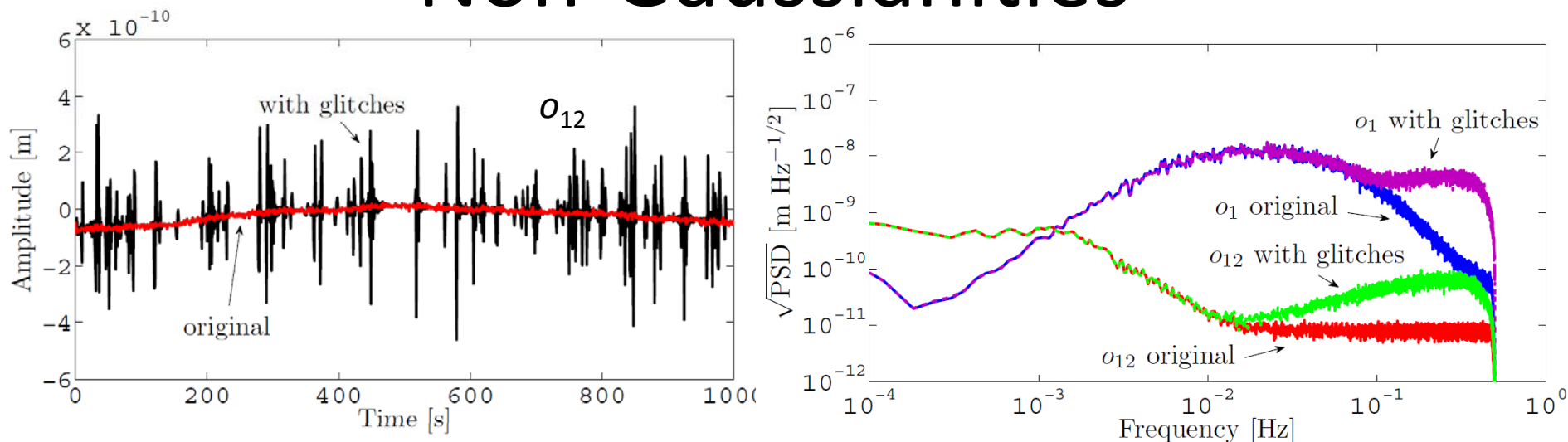
abs. deviation, log-normal distr.

log. deviation, Lorentzian distr.

Better weighting for large deviations than squared and abs dev.



Non-Gaussianities



Parameter	Real	Best-fit		Best-fit		Best-fit		Guess
		(mean sq. dev.)	(mean log. dev.)	(mean sq. dev.)	(mean log. dev.)	(mean sq. dev.)	(mean log. dev.)	
		$\chi^2 = 10$		$\chi^2 = 2.1$		$\chi^2 = 0.95$		
$\omega_1^2 [10^{-6} \text{ s}^{-2}]$	-1.32	-1.320(1)	{0.061}	-1.3188(6)	{2.0}	-1.3192(4)	{2.0}	-1.3
$\omega_{12}^2 [10^{-6} \text{ s}^{-2}]$	-0.68	-0.6798(7)	{0.29}	-0.68000(3)	{0.011}	-0.6804(2)	{1.8}	-0.7
$S_{21} [10^{-4}]$	1.1	1.10(2)	{0.074}	1.113(7)	{1.8}	1.116(5)	{3.4}	0
A_{df}	1.01	1.011(3)	{0.29}	1.010(1)	{0.23}	1.0109(8)	{1.2}	1
A_{sus}	0.99	0.99000(5)	{0.035}	0.98959(2)	{20}	0.99001(1)	{0.99}	1
$\Delta t_1 [\text{s}]$	0.1	0.100(3)	{0.045}	0.090(1)	{8.3}	0.1007(8)	{0.90}	0
$\Delta t_{12} [\text{s}]$	0.1	0.098(5)	{0.36}	-0.0290(2)	{58}	0.098(2)	{1.2}	0

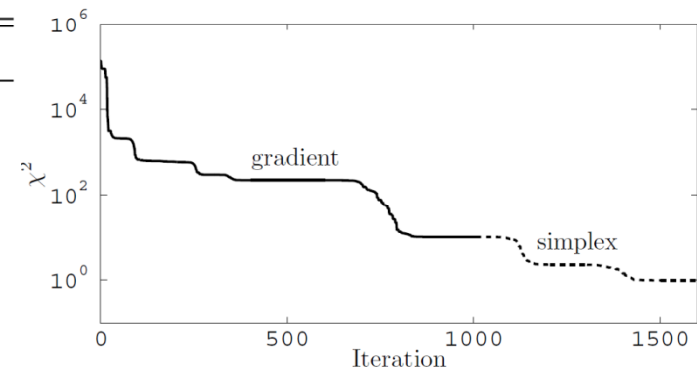
- χ^2 regularizes toward ~ 1
- the parameter bias, in average, tends to < 3

Under-performing actuators under-estimated couplings

Investigated the case of a miscalibrated LPF mission, in which:

- the TM couplings are stronger than one may expect
- the (thruster and capacitive) actuators have an appreciable loss of efficiency

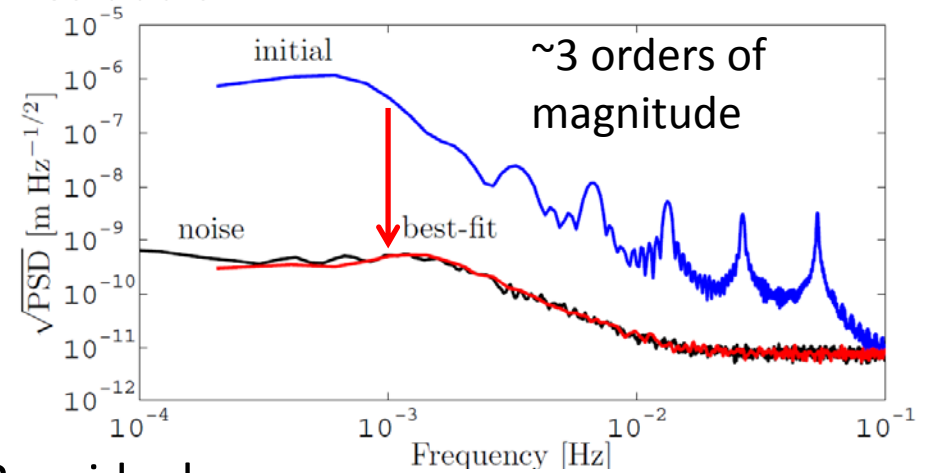
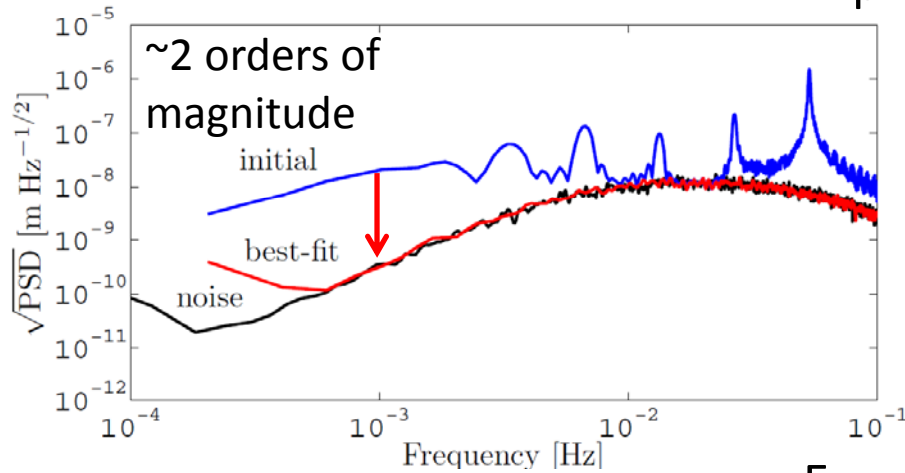
Parameter	True	Best-fit		Guess	
$\omega_1^2 [10^{-6} \text{ s}^{-2}]$	-3	-2.9998(2)	{1.1}	-1.3	$\{7.8 \times 10^3\}$
$\omega_{12}^2 [10^{-6} \text{ s}^{-2}]$	-2	-2.0000(1)	{0.32}	-0.7	$\{1.0 \times 10^4\}$
$S_{21} [10^{-3}]$	-1.5	-1.4998(1)	{0.55}	0	$\{4.7 \times 10^3\}$
A_{df}	0.62	0.61994(8)	{0.77}	1	$\{4.9 \times 10^3\}$
A_{sus}	0.6	0.599990(8)	{1.3}	1	$\{5.1 \times 10^4\}$
$\Delta t_1 [\text{s}]$	0.6	0.6013(7)	{1.8}	0	$\{8.4 \times 10^2\}$
$\Delta t_{12} [\text{s}]$	0.4	0.398(2)	{0.95}	0	$\{2.3 \times 10^2\}$



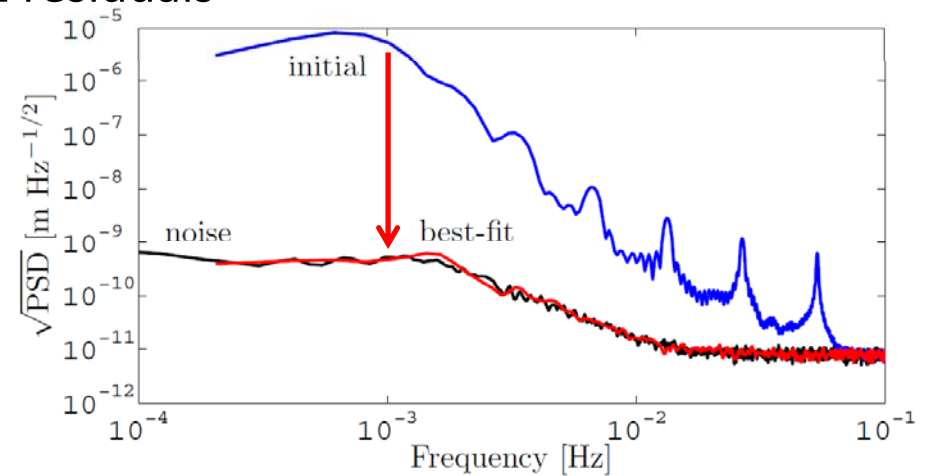
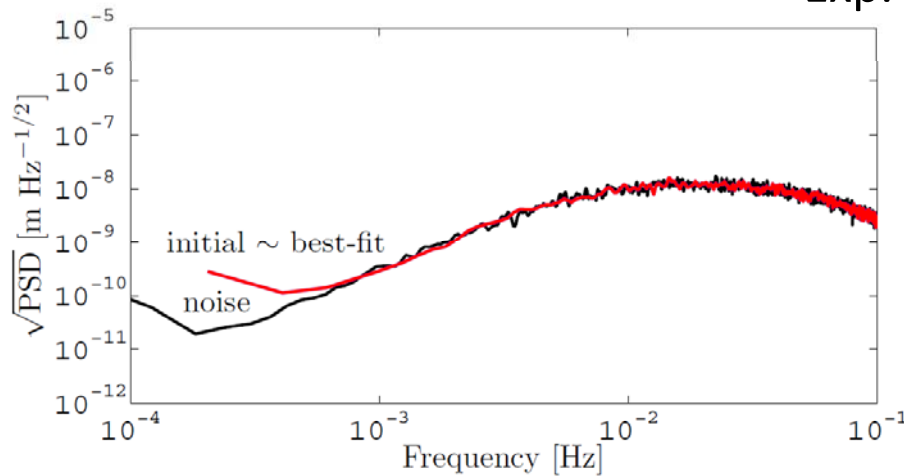
**The parameter bias reduces from 10^3 - $10^4 \sigma$ to <2 and
the χ^2 from $\sim 10^5$ to ~ 1**

Under-performing actuators under-estimated couplings

Exp. 1 residuals



Exp. 2 residuals



Equivalent acceleration noise

Inaccuracies in the estimated system parameters produce **systematic errors** in recovered equivalent acceleration noise

$$\delta S_{n,f} \simeq \delta \Delta S_{n,o} \Delta^* + \Delta S_{n,o} \delta \Delta^*$$

PSD matrix of the sensed relative motion

inaccuracies of the diff. operator

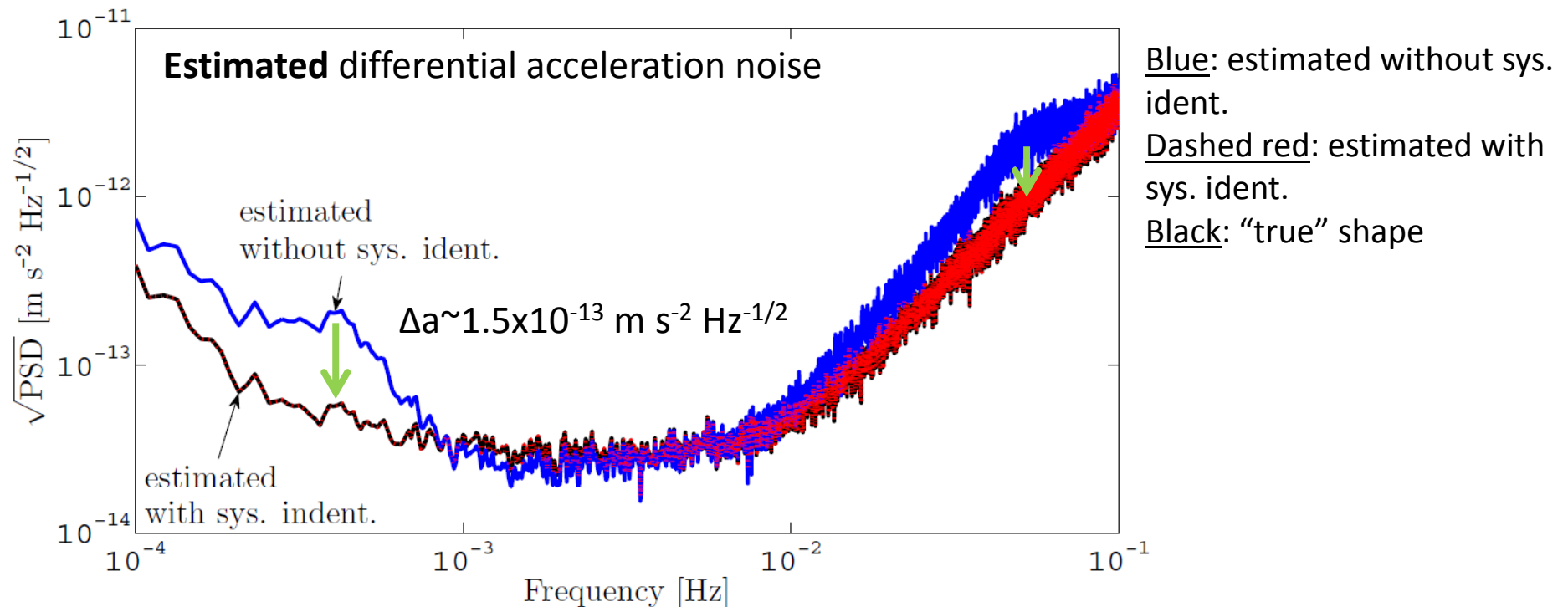
“true” diff. operator, as with the perfect knowledge of the system

systematic errors in the estimated equivalent acceleration noise

Perform an estimation of the equivalent acceleration noise in a miscalibrated LPF mission (as in the previous example):

- **without** a system identification (@ initial guess)
- **with** a system identification (@ best-fit)
- with the perfect knowledge of the system (@ true)

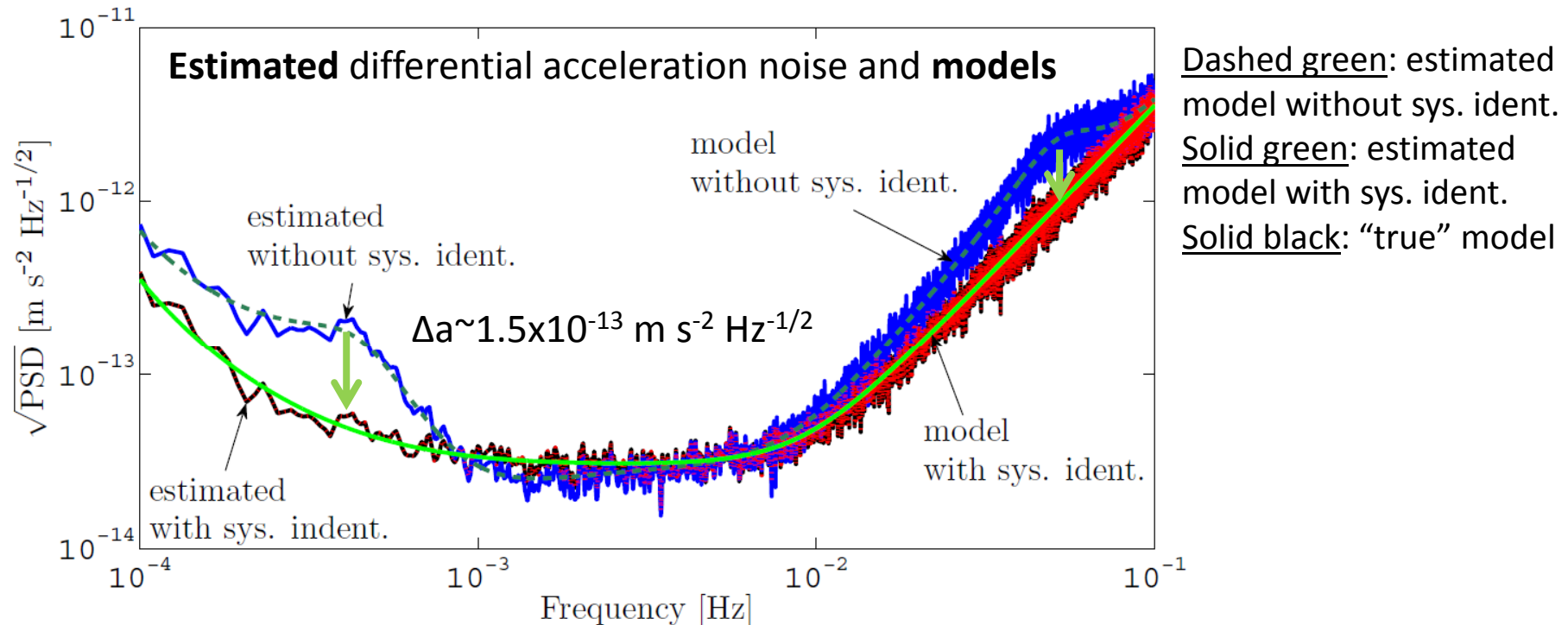
Equivalent acceleration noise



Thanks to system identification:

- the estimated acceleration recovers the "true" shape
- **improvement of a factor ~ 2 around 50 mHz**
- **improvement of a factor ~ 4 around 0.4 mHz**

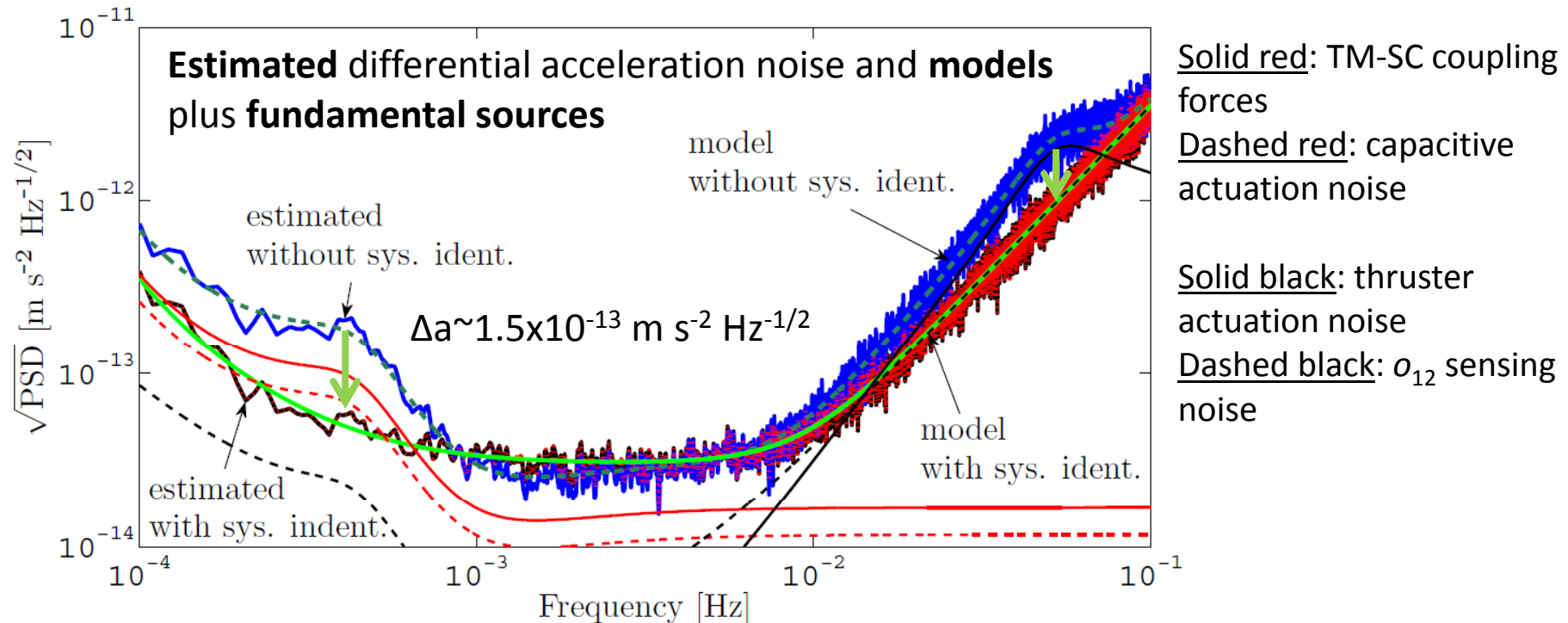
Equivalent acceleration noise



The agreement between estimated noise and models shows:

- the models **explain** the estimated acceleration spectra
- the **accuracy** of the noise generation

Equivalent acceleration noise

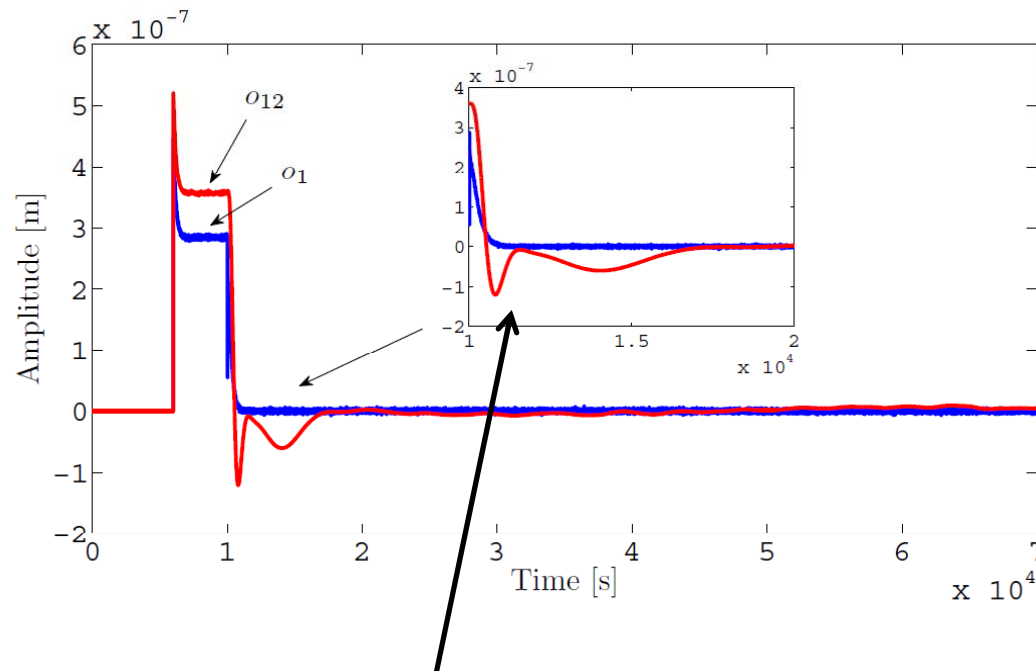


The systematic errors are due to:

- 0.4 mHz, uncalibrated coupling forces (ω_1^2 and ω_2^2) and capacitive actuation (A_{sus})
- 50 mHz, uncalibrated thruster actuation (A_{df}) and sensing noise (S_{21})

Suppressing transients in the acceleration noise

As a consequence of changes of state and **non-zero initial conditions**, the presence of transients in the data is an expected behavior.

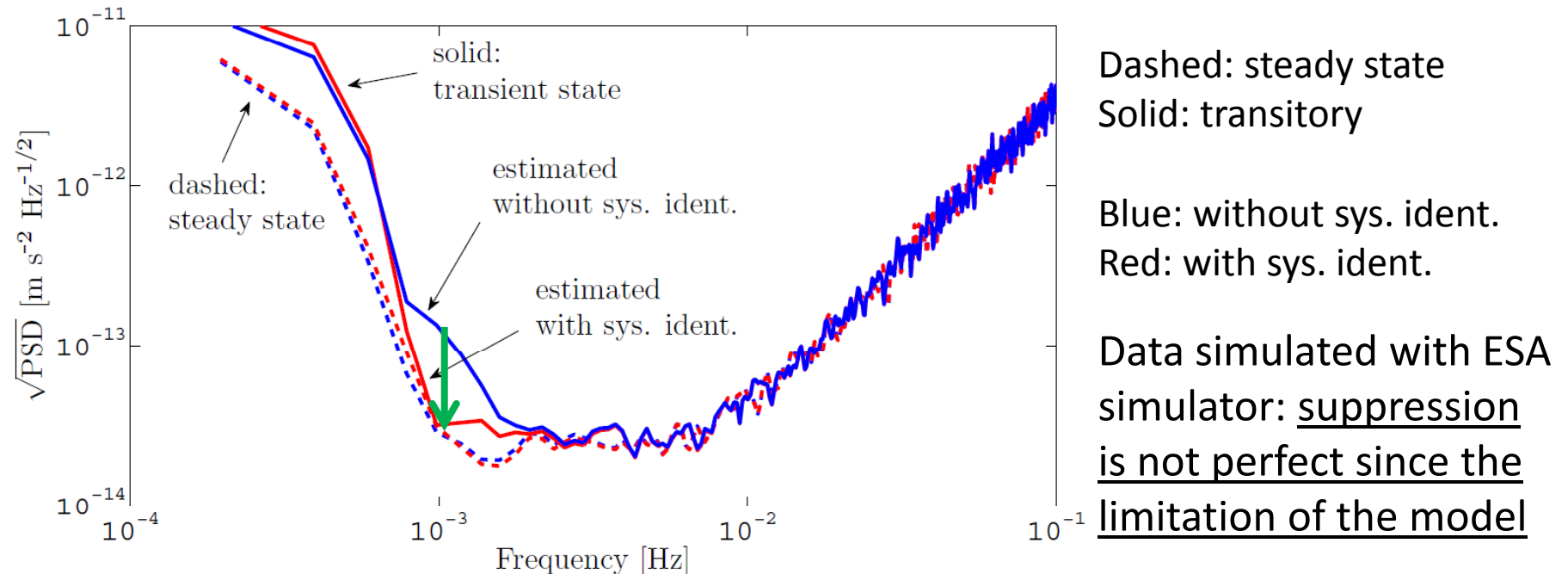


Transients last for about 2 hours in o_{12}

Suppressing transients in the acceleration noise

Comparison:

- (i) between the acceleration estimated **at the transitory** (first 3×10^4 s) and **steady state**;
- (ii) between the acceleration estimated **without and with system identification**



System identification helps in mitigating the transitory in the estimated acceleration noise

Design of optimal experiments

Goal: find optimal experiment designs allowing for an **optimal determination of the system parameters**

The LPF experiments can be optimized within the system constraints:

- shape of the input signals
- sensing range of the interferometer $100 \mu\text{m}$
- thruster authority $100 \mu\text{N}$
- capacitive authority 2.5 nN

$$o_i(t) = \sum_{n=1}^{N_{\text{inj}}} a_n \sin(2\pi f_n t) \theta(t - t'_n) \theta(t''_n - t)$$

input signals: series of sine waves with **discrete frequencies** (we require **integer number of cycles**)

- $T < 3\text{h}$ (experiment duration): fixed
- $N_{\text{inj}} = 7$: fixed to meet the exp. duration
- $\delta t = 1200 \text{ s}$ (duration of each sine wave): fixed
- $\delta t_{\text{gap}} = 150 \text{ s}$ (gap between two sine waves): fixed for transitory decay
- f_n (injection freq.): **optimized**
- a_n (injection ampl.): varied according to f_n and the (sensing/actuation) constraints

Design of optimal experiments

Fisher information matrix

$$\mathcal{J}(\theta) = \int o_i(\omega, \theta)^* \nabla_p T_{o_i \rightarrow o}(\omega, p_{\text{est}})^* S_n(\omega)^{-1} \nabla_p T_{o_i \rightarrow o}(\omega, p_{\text{est}}) o_i(\omega, \theta) d\omega$$

input parameters (injection frequencies)

noise cross PSD matrix

estimated system parameters

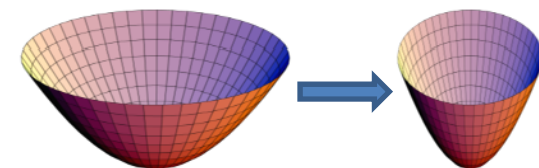
input signals being optimized

modeled transfer matrix *with* system identification

Perform (non-linear discrete) optimization of the scalar estimator

$$\phi(\theta) = \begin{cases} \det(\mathcal{J}(\theta)) \\ \min(\text{eig}(\mathcal{J}(\theta))) \\ \text{tr}(\mathcal{J}(\theta)) \end{cases}$$

optimization criteria



minimizes "covariance volume"

Design of optimal experiments

Parameter	Standard		Optimal	
st. dev.	Exp. 1 & Exp. 2		Exp. 1 & Exp. 2	
$\sigma_{\omega_1^2}$ [s ⁻²]	4×10^{-10}	{1.4}	2×10^{-10}	{0.68}
$\sigma_{\omega_{12}^2}$ [s ⁻²]	2×10^{-10}	{0.41}	1×10^{-10}	{2.0}
$\sigma_{S_{21}}$	4×10^{-7}	{0.086}	1×10^{-7}	{1.1}
$\sigma_{A_{df}}$	7×10^{-4}	{1.6}	1×10^{-4}	{0.50}
$\sigma_{A_{sus}}$	1×10^{-5}	{1.7}	2×10^{-6}	{0.28}

Correlation	Standard	Optimal
Corr[S_{21}, ω_{12}^2]	-0.2	-0.03
Corr[S_{21}, ω_1^2]	0.09	0.02
Corr[A_{sus}, ω_1^2]	-0.7	-0.2
Corr[$\omega_1^2, \omega_{12}^2$]	-0.5	-0.5

With the optimized design:

- Improvement in precision:
 - factor 2 for ω_1^2 and ω_{12}^2
 - factor 4 for S_{21}
 - factor 5-7 for A_{sus}, A_{df} : important for compensating the SC jitter
- Some parameters show lower correlation than the standard experiments
- The optimization converged to only two injection frequencies (0.83 mHz, 50 mHz)

Concluding remarks

- Theoretical contribution to the foundations of spacetime metrology with the LPF differential accelerometer
- Modeling of the dynamics of the LISA arm implemented in LPF
- Development of the parameter estimation method employed for system calibration and subtraction of different effects
- Relevance of system identification for LPF

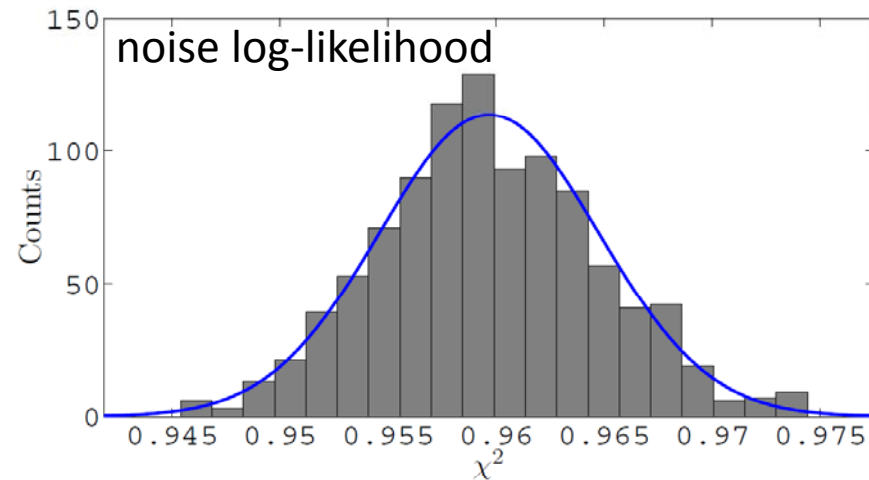
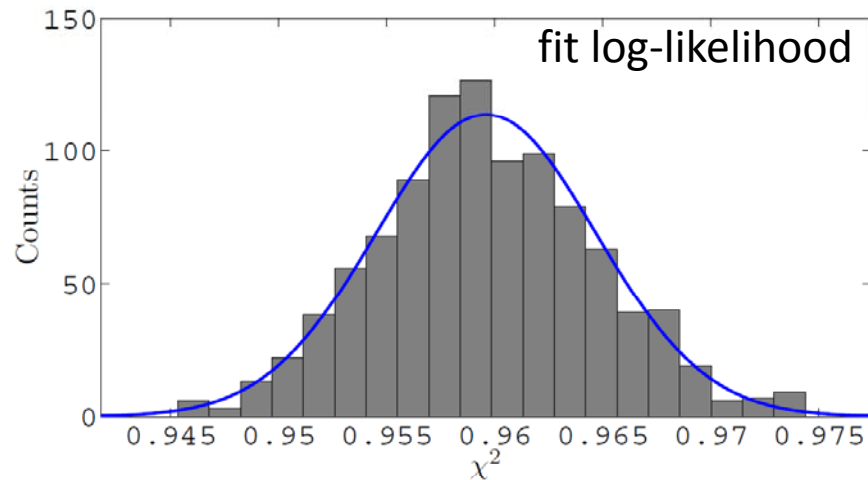
Future perspectives

- More investigation in the reformulation of the Doppler link as a differential accelerometer
- Application of system identification to the analysis of some cross-talk experiments
- Investigation of non-stationary (transient) components in the noise
- Application of the proposed optimal design to the ESA simulator
- Currently under investigation, the application of system identification in the domain of equivalent acceleration

Thanks for your attention!

Additional slides...

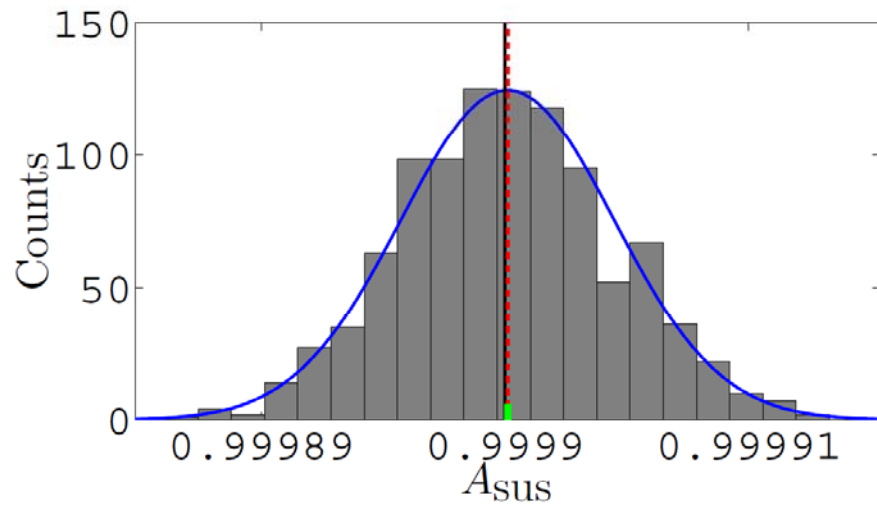
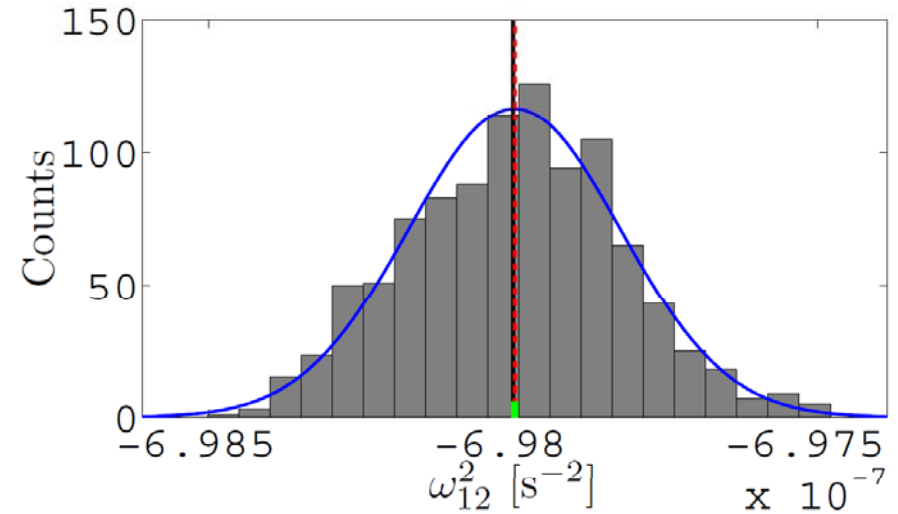
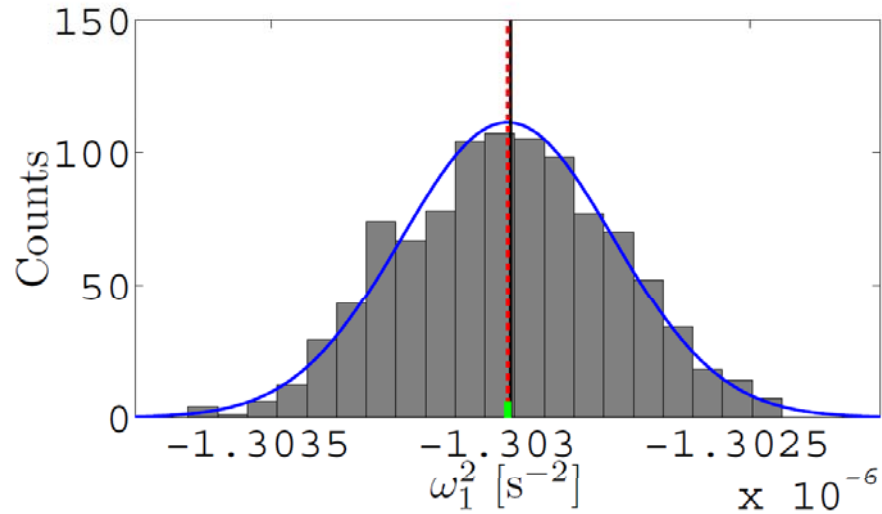
Monte Carlo validation



1000 noise realizations, true (7) parameters kept fixed

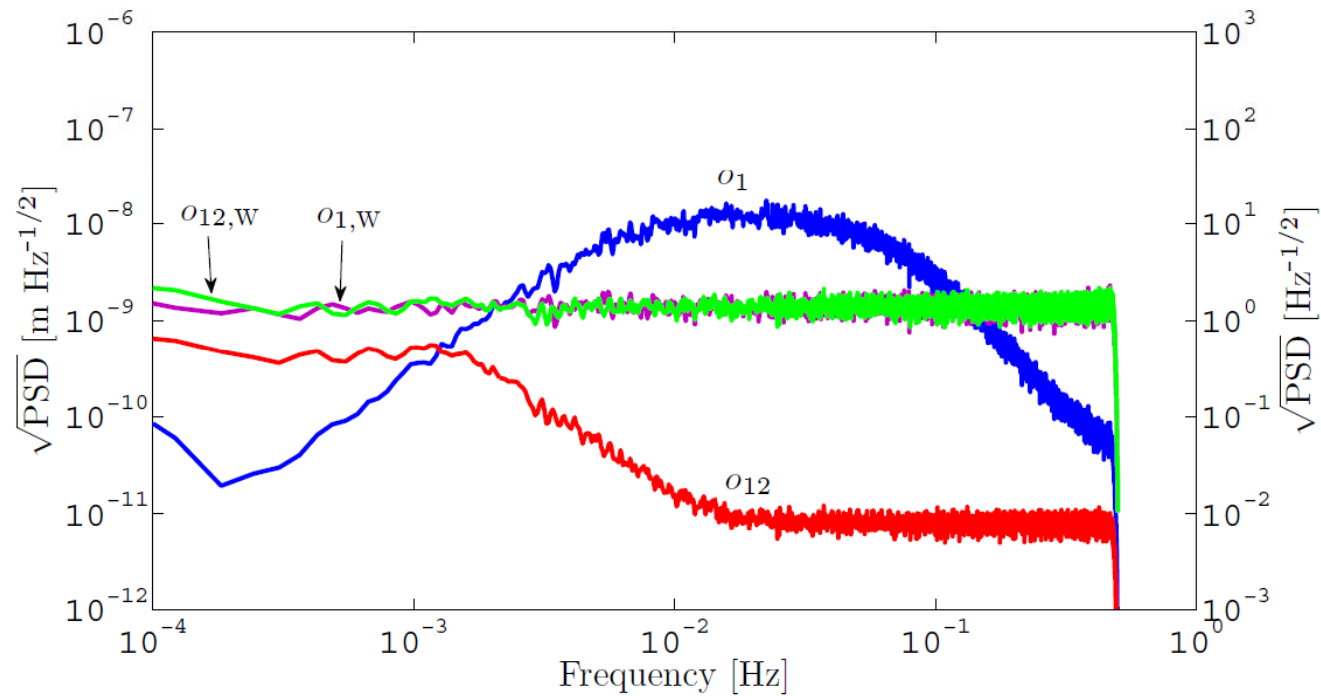
- all parameters are in good agreement with a Gaussian PDF, as well as correlations and variances
- parameters are unbiased to within 1-2 standard deviations
- expected (Fisher) errors are approximately in agreement with the noise fluctuation
- the method statistically suppresses the signals (see above)

Monte Carlo validation



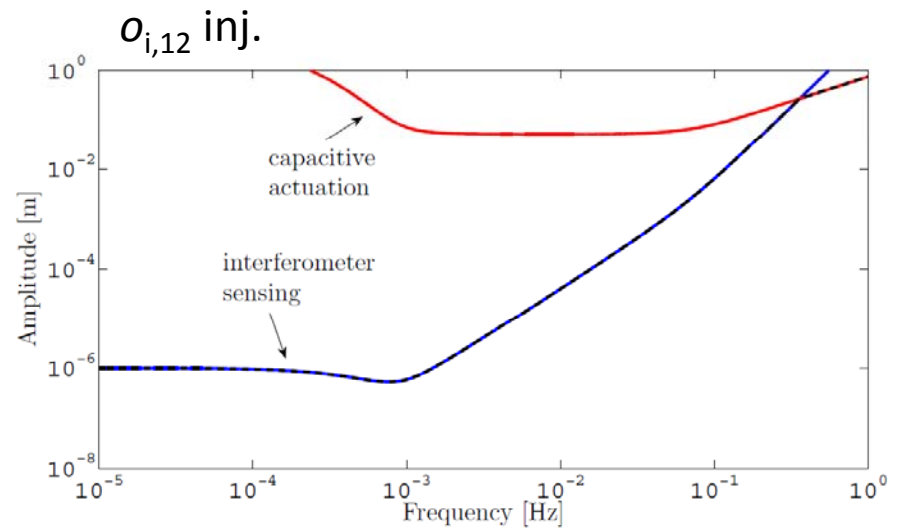
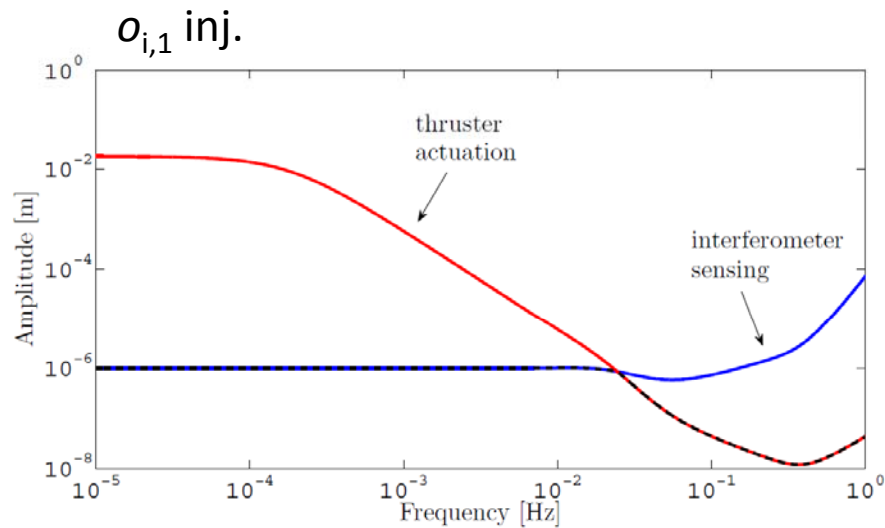
Parameter	True	Mean best-fit	Best-fit st. dev.	Mean exp. st. dev.
$\omega_1^2 [10^{-6} \text{ s}^{-2}]$	-1.303	-1.303006(7)	2×10^{-4}	1×10^{-3}
$\omega_{12}^2 [10^{-6} \text{ s}^{-2}]$	-0.698	-0.697998(6)	2×10^{-4}	5×10^{-4}
$S_{21} [10^{-4}]$	0.9	0.90004(9)	3×10^{-3}	4×10^{-3}
A_{df}	1.003	1.00297(1)	4×10^{-4}	4×10^{-4}
A_{sus}	0.9999	0.9999001(1)	4×10^{-6}	2×10^{-5}
$\Delta t_1 [\text{s}]$	0.06	0.059995(3)	9×10^{-5}	3×10^{-4}
$\Delta t_{12} [\text{s}]$	0.05	0.05000(3)	8×10^{-4}	1×10^{-3}

Whitening



System identification relies upon a proper estimation of whitening filters

Design of optimal experiments



For almost the entire frequency band, the maximum amplitudes are limited by the interferometer sensing

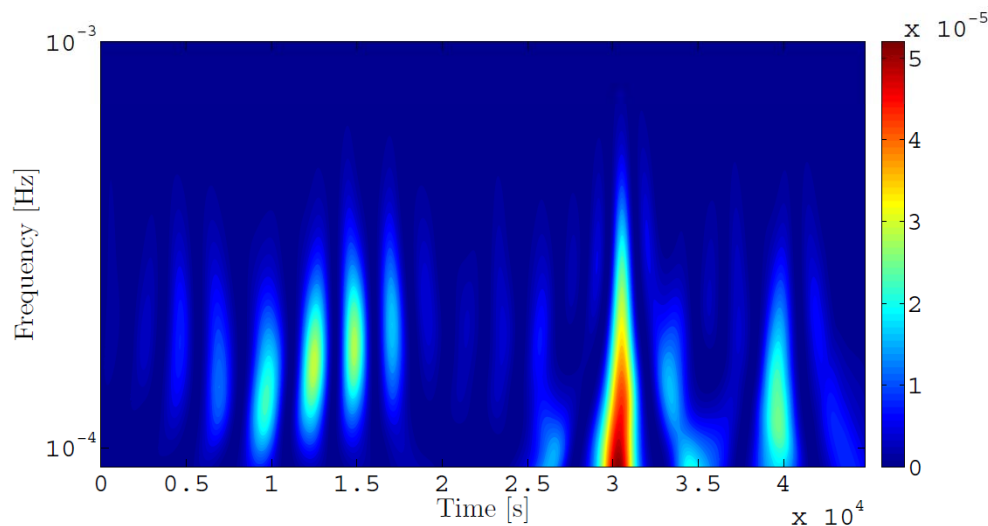
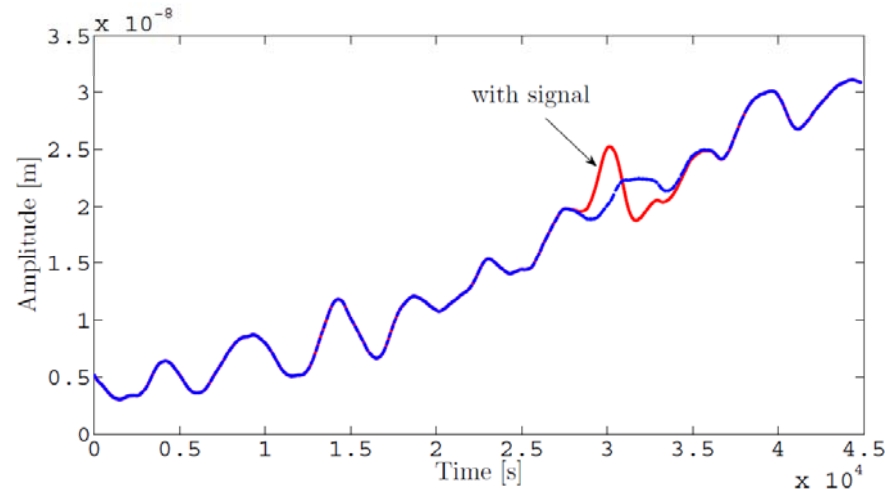
Identification in the acceleration domain

$$\begin{aligned}\chi^2 &= \int (f_{\text{exp}} - f_{\text{mdl}})^* S_{n,f}^{-1} (f_{\text{exp}} - f_{\text{mdl}}) d\omega \\ &= \int (o_{\text{exp}} - o_{\text{mdl}})^* \Delta^* (\Delta^{*-1} S_{n,o}^{-1} \Delta^{-1}) \Delta (o_{\text{exp}} - o_{\text{mdl}}) d\omega \\ &= \int (o_{\text{exp}} - o_{\text{mdl}})^* S_{n,o}^{-1} (o_{\text{exp}} - o_{\text{mdl}}) d\omega\end{aligned}$$

Comment: formally equivalent to standard identification in displacement, but the transitory is mitigated in equivalent acceleration.

Implementation: closed-loop optimization where the parameters enter into the estimated acceleration

Transient analysis



- injected a (Gaussian) force signal of amplitude $1.6 \times 10^{-13} \text{ ms}^{-2}$ and duration $\sim 1 \text{ h}$
- PSD estimation does not detect any (statistically significant) excess
- time-frequency wavelet spectrogram: a factor >2 noise excess
- can be applied to the search of transients in LPF noise, like “modified gravity” signals